According to Hepatitis C Virus (HCV) Infection Stage, Interleukin-7 Plus 4-1BB Triggering Alone or Combined with PD-1 Blockade Increases TRAF1^{low} HCV-Specific CD8$^+$ Cell Reactivity

Elia Moreno-Cubero,[a,b] Dolores Subirá,[c] Eduardo Sanz-de-Villalobos,[a] Trinidad Parra-Cid,[d] Antonio Madejón,[e] Joaquín Miquel,[a] Antonio Olveira,[e] Alejandro González-Praetorius,[f] Javier García-Samaniego,[e] (ORCID) Juan-Ramón Larrubia[a,g]

[a]Translational Hepatology Unit, Section of Digestive Diseases, Hospital Universitario de Guadalajara, Guadalajara, Spain
[b]Department of Biology of Systems, University of Alcalá, Madrid, Spain
[c]Service of Hematology, Hospital Universitario de Guadalajara, Guadalajara, Spain
[d]Service of Biochemistry, Hospital Universitario de Guadalajara, Guadalajara, Spain
[e]Liver Unit, Hospital Universitario La Paz, CIBERehd, IdiPaz, Madrid, Spain
[f]Service of Microbiology, Hospital Universitario de Guadalajara, Guadalajara, Spain
[g]Department of Medicine and Medical Specialties, University of Alcalá, Madrid, Spain

ABSTRACT Hepatitis C virus (HCV)-specific CD8$^+$ T cells suffer a progressive exhaustion during persistent infection (PI) with HCV. This process could involve the positive immune checkpoint 4-1BB/4-1BBL through the loss of its signal transducer, TRAF1. To address this issue, peripheral HCV-specific CD8$^+$ T cells (pentamer-positive [pentamer$^+$]/CD8$^+$ T cells) from patients with PI and resolved infection (RI) after treatment were studied. The duration of HCV infection and the liver fibrosis progression rate inversely correlated with the likelihood of detection of peripheral pentamer$^+$/CD8$^+$ cells. In PI, pentamer$^+$/CD8$^+$ cells had impaired antigen-specific reactivity that worsened when these cells were not detectable *ex vivo*. Short/midduration PI was characterized by detectable peripheral PD-1$^+$ CD127^{low} TRAF1^{low} cells. After triggering of T cell receptors (TCR), the TRAF1 level positively correlated with the levels of CD127, Mcl-1, and CD107a expression and proliferation intensity but negatively with PD-1 expression, linking TRAF1^{low} to exhaustion. *In vitro* treatment with interleukin-7 (IL-7) upregulated TRAF1 expression, while treatment with transforming growth factor-β1 (TGF-β1) did the opposite, suggesting that the IL-7/TGF-β1 balance, besides TCR stimulation, could be involved in TRAF1 regulation. In fact, the serum TGF-β1 concentration was higher in patients with PI than in patients with RI, and it negatively correlated with TRAF1 expression. In line with IL-7 increasing the level of TRAF1 expression, IL-7 plus 4-1BBL treatment *in vitro* enhanced T cell reactivity in patients with short/midduration infection. However, in patients with long-lasting PI, anti-PD-L1, in addition to the combination of IL-7 and 4-1BBL, was necessary to reestablish T cell proliferation in individuals with slowly progressing liver fibrosis (slow fibrosers) but had no effect in rapid fibrosers. In conclusion, a peripheral hyporeactive TRAF1^{low} HCV-specific CD8$^+$ T cell response, restorable by IL-7 plus 4-1BBL treatment, characterizes short/midduration PI. In long-lasting disease, HCV-specific CD8$^+$ T cells are rarely detectable *ex vivo*, but treatment with IL-7, 4-1BBL, and anti-PD-L1 recovers their reactivity *in vitro* in slow fibrosers.

IMPORTANCE Hepatitis C virus (HCV) infects 71 million people worldwide. Two-thirds develop a chronic disease that can lead to cirrhosis and hepatocellular carcinoma. Direct-acting antivirals clear the infection, but there are still patients who relapse. In these cases, additional immunotherapy could play a vital role. A successful

anti-HCV immune response depends on virus-specific CD8$^+$ T cells. During chronic infection, these cells are functionally impaired, which could be due to the failure of costimulation. This study describes exhausted specific T cells, characterized by low levels of expression of the signal transducer TRAF1 of the positive costimulatory pathway 4-1BB/4-1BBL. IL-7 upregulated TRAF1 expression and improved T cell reactivity in patients with short/midduration disease, while in patients with long-lasting infection, it was also necessary to block the negative PD-1/PD-L1 checkpoint. When the results are taken together, this work supports novel ways of restoring the specific CD8$^+$ T cell response, shedding light on the importance of TRAF1 signaling. This could be a promising target for future immunotherapy.

Hepatitis C virus (HCV)-specific CD8$^+$ T cells are vital for the clearance of HCV [1] and might play a role in the avoidance of relapses because of the temporary presence of trace levels of occult virus after the treatment-induced control of HCV infection [2–7]. Nevertheless, during persistent infection (PI) with HCV, this response either is exhausted or is even deleted [8–11]. Several strategies have focused on the modulation of immune checkpoints to restore *in vitro* T cell reactivity and have had variable success [8, 12, 13]. The progenitor T cell pool could be a sound candidate as a subset responsive to immunotherapeutic approaches [14, 15]. However, it has been shown that this population can develop a gradient of functional impairment according to the infection stage [16, 17]. During PI, the presence of peripheral HCV-specific CD8$^+$ T cells at a frequency below the detection threshold of conventional methods [18] might suggest deletion of the terminal effector memory population and an intense impairment of the progenitor subset, while the presence of detectable cells could be linked to less severe exhaustion [9, 15, 16]. Therefore, an immunomodulatory strategy to restore T cell numbers could yield different results, according to whether the detection of peripheral HCV-specific T cells *ex vivo* is possible or not.

The triggering of the immune checkpoint tumor necrosis factor (TNF) receptor superfamily member 9 (4-1BB)/4-1BB ligand (4-1BBL) [19] to improve the HCV-specific CD8$^+$ T cell response has already been tested, but unfortunately, it was shown to have weak efficacy [13]. This failure could be due to the impairment of signal transduction. TNF receptor-associated factor 1 (TRAF1) is the key transducer of this pathway [20]. TRAF1 levels are low in resting cells but are upregulated via NF-κB after T cell activation [21, 22]. TRAF1 loss is observed during some chronic viral infections, such as those with murine lymphocytic choriomeningitis virus (LCMV) [23]. Of note, besides triggering T cell receptors (TCR), interleukin-7 (IL-7) upregulates TRAF1 expression during LCMV infection, while triggering of transforming growth factor-β1 (TGF-β1) does the opposite [23]. Several mechanisms could be involved in inducing TGF-β1 secretion during chronic HCV infection [24–26], and consequently, the induction of TGF-β1 secretion could affect TRAF1 expression. Thus, IL-7 could potentially be utilized [27] to restore TRAF1 levels by counteracting the effect of TGF-β1 in those exhausted T cells not able to upregulate TRAF1 after TCR stimulation. The role of IL-7 in TRAF1 expression in HCV-specific CD8$^+$ T cells during PI has not been studied before. Our work shows that during short/midduration infection, exhausted TRAF1^{low}-expressing HCV-specific CD8 T cells are generally detectable in the peripheral compartment and are amenable to IL-7 plus 4-1BB triggering. On the contrary, during long-lasting disease, these cells are commonly present at levels below the direct detection threshold *ex vivo* and the additional blockade of the programmed cell death protein 1 (PD-1) checkpoint is necessary to restore their reactivity. These findings provide novel insight into the role of TRAF1 in the functional impairment of HCV-specific CD8$^+$ T cells, which could open new opportunities for those patients not responding to direct-acting antivirals (DAA) [28] as well as patients with other chronic viral infections and cancer.

TABLE 1 Features of the patients enrolled in the study[a]

Characteristic	Value(s) for:		
	RI group (n = 42)	PI group (n = 35)	P value
Median (IQR) age (yr)	57 (13)	55 (13)	NS[b]
% of male patients	67	63	NS[c]
Median (IQR) duration of infection (yr)	34 (12)	36 (12)	NS[b]
% of patients with HLA-A2	100	100	NS[c]
% of patients infected with HCV genotype 1	100	100	NS[c]
% of patients with the following source of infection:			
Unknown	12	6	NS[c]
IVDA	5	9	NS[c]
Other[d]	83	85	NS[c]
No. of patients previously treated with:			
No treatment	0	20	NA
P-IFN + RBV	11	12	NA
P-IFN + RBV + DAA	12	3	NA
DAA regimen	19	0	NA
Median (IQR) HCV viral load (IU · ml^{-1}, log scale)	UDL	6.2 (0.79)	<0.001[b]
Median (IQR) ALT concn (IU · ml^{-1})	17 (7)	47 (73)	<0.001[b]
% of patients with the following degree of liver fibrosis[e]:			
F0 to F2	43	57	NS[c]
F3 or F4	57	43	
% of patients with the following fibrosis speed:			
Slow (≤0.06 unit · year^{-1})	31	37	NS[c]
Mid/rapid (>0.06 unit · year^{-1})	69	63	
No. of patients with the following NS3$_{1073}$ sequence:			
WT	ND	24	NA
EV	ND	0	NA
Unknown	ND	11	NA
No. of patients with the following NS3$_{1406}$ sequence:			
WT	ND	14	NA
EV	ND	6	NA
Unknown	ND	12	NA

[a]ALT, alanine aminotransferase; DAA, direct-acting antiviral; EV, escape variant; IQR, interquartile range; IVDA, intravenous drug abuse; NA, not applicable; NS, nonsignificant; ND, not done; P-IFN, pegylated alpha2 interferon; PI, persistent infection; RBV, ribavirin; RI, resolved infection; UDL, under the detection limit; WT, wild type.
[b]Determined by the Mann-Whitney U test.
[c]Determined by the chi-square test.
[d]Parenteral nonintravenous drug abuse or sexual transmission.
[e]The degree of liver fibrosis was estimated by transient elastography or liver biopsy.

RESULTS

***Ex vivo* pentamer-positive (pentamer$^+$)/CD8$^+$ cell detection correlates with the duration of HCV infection and the liver fibrosis progression rate.** The groups with RI and PI displayed comparable demographic and clinical features (Table 1). In both groups, peripheral blood lymphocytes (PBL) were tested for the presence of CD8$^+$ T cells specific for two human leukocyte antigen (HLA)-A2-restricted HCV genotype 1 NS3 epitopes. Sequencing of the epitope consisting of HCV NS3 from positions 1073 to 1081 (NS3$_{1073-1081}$; also referred to here as the NS3$_{1073}$ epitope) and the epitope consisting of HCV NS3 from positions 1406 to 1415 (NS3$_{1406-1415}$; also referred to here as the NS3$_{1406}$ epitope) could be performed for 66% of the patients with PI. Remarkably, the sequences of 100% of the NS3$_{1073}$ epitopes and 70% of the NS3$_{1406}$ epitopes tested were similar to those of the peptides loaded into the pentamers (Table 2). As HCV isolates from patients with RI were not available for sequencing, due to a lack of pretreatment serum samples, in order not to bias the analysis, all samples were

TABLE 2 NS3 epitope sequence in selected patients with persistent genotype 1 infection and its correlation with *ex vivo* detection and the reactivity of HCV-specific CD8+ cells according to liver fibrosis and disease duration[a]

Duration of infection and degree of liver fibrosis	ID	Degree of liver fibrosis	Duration (yr)	Genotype	Results for HCV NS3$_{1073}$ peptide				Results for HCV NS3$_{1406}$ peptide			
					NS3$_{1073}$ sequence compared to that in Pent (CINGVCWTV)[b]	Ex vivo detection of cells[c]	Ag-specific proliferation with: No treatment	4-1BBL + IL-7 treatment	NS3$_{1406}$ sequence compared to that in Pent (KLVALGINAV)[b]	Ex vivo detection of cells[c]	Ag-specific proliferation with: No treatment	4-1BBL + IL-7 treatment
≤40 yr												
F0 to F2	272P	F2	40	1a	--S------	0.02	0.6	0.17	-----V----	0.04	8.6	3.7
	273P	F1	32	1a	ND		Neg		----------	Neg	Neg	Neg
	316P	F1	35	1a	---------	0.02	Neg	0.29	----------	Neg	Neg	0.12
	376P	F1	40	1b	---------	0.02	0.08	ND	ND			
	635P	F1	30	1a	---------	0.02	ND	ND	---M-V----	0.03	Neg	5.05
	684P	F2	28	1a	---------	Neg	Neg	Neg	ND		Neg	Neg
	1090P	F2	21	1b	---------	Neg	Neg	Neg	----------			
	1208P	F2	35	1a	---------	Neg	4.6	0.45	---------	Neg	Neg	0.48
	1245P	F1	34	1a	---------	0.05	0.6	1.8	---------	Neg	0.1	0.2
	1270P	F2	28	1a	---------	Neg	Neg	Neg	----V-----	Neg	Neg	Neg
F3 or F4	442P	F3	28	1a	---------	0.02	1.8	1.1	--G--L----	Neg	0.7	0.3
	516P	F3	33	1a	---------	0.04	2.3	3.35	--G--L----	Neg	Neg	Neg
	1024P	F4	40	1a	---------	Neg	0.32	ND	----V-----	Neg	Neg	0.78
	1045P	F4	34	1a	---------	Neg	Neg		--AG--M---	Neg	ND	ND
	1058P	F3	30	1a	---------	0.04	2.89	1.14	---M-V----	0.14	6.5	4.4
	1094P	F3	32	1b	-V-------	Neg	Neg	0.17	ND			
	1165P	F4	28	1a	---------	0.02	Neg	ND	-----V----	0.03	Neg	ND
No. positive/total no. (%)[d]						9/16 (56%)	8/14 (57%)	8/11 (73%)		2/9 (22%)	2/9 (22%)	5/8 (63%)
>40 yr												
F0 to F2	450P	F2	41	1b	---------	Neg	Neg	Neg	ND			
	1064P	F1	42	1a	---------	Neg	Neg	ND	--G-------	Neg	0.18	Neg
F3 or F4	33P	F3	41	1a	-V-------	Neg	Neg	Neg	---------	Neg	Neg	Neg
	380P	F4	49	1a	---------	Neg	Neg	ND	---------	Neg	Neg	ND
	969P	F3	41	1a	---------	Neg	Neg	Neg	---------	Neg	Neg	Neg
	727P	F3	63	1a	---------	Neg	Neg	Neg	-----V----	Neg	Neg	Neg
	1200P	F3	48	1a	---------	Neg	Neg	Neg	------V---	Neg	Neg	1.3
No. positive/total no. (%)[d]						0/7 (0%)	0/7 (0%)	0/5 (0%)		0/5 (0%)	0/5 (0%)	1/4 (25%)

[a]Ag-specific proliferation (%), proliferation after 10 days of specific *in vitro* challenge in the presence of 4-1BBL plus IL-7 treatment (4-1BBL + IL-7) and in the absence of 4-1BBL plus IL-7 treatment (no treatment); Duration, duration of HCV infection; ID, patient identification; ND, not done; Neg, negative; Pent, HLA-I/pentameric peptide complexes. Shading indicates the escape variants not cross-recognized by wild-type-primed T cells. The underlined data highlight the cases with increased proliferation after IL-7 plus 4-1BBL treatment.
[b]A hyphen indicates that the sequences is the same as that in the pentamer.
[c]The frequency of NS3 pentamer-binding CD8+ cells out of the number of total CD8+ cells (in percent; data are highlighted in bold when the value is higher than the detection threshold).
[d]The data represent the number of patients with positive data/total number of patients (percent), but only those patients infected with HCV isolates with sequences similar to the peptide sequence loaded in the pentamers are included in the calculation.

(A)

(C)

(B)
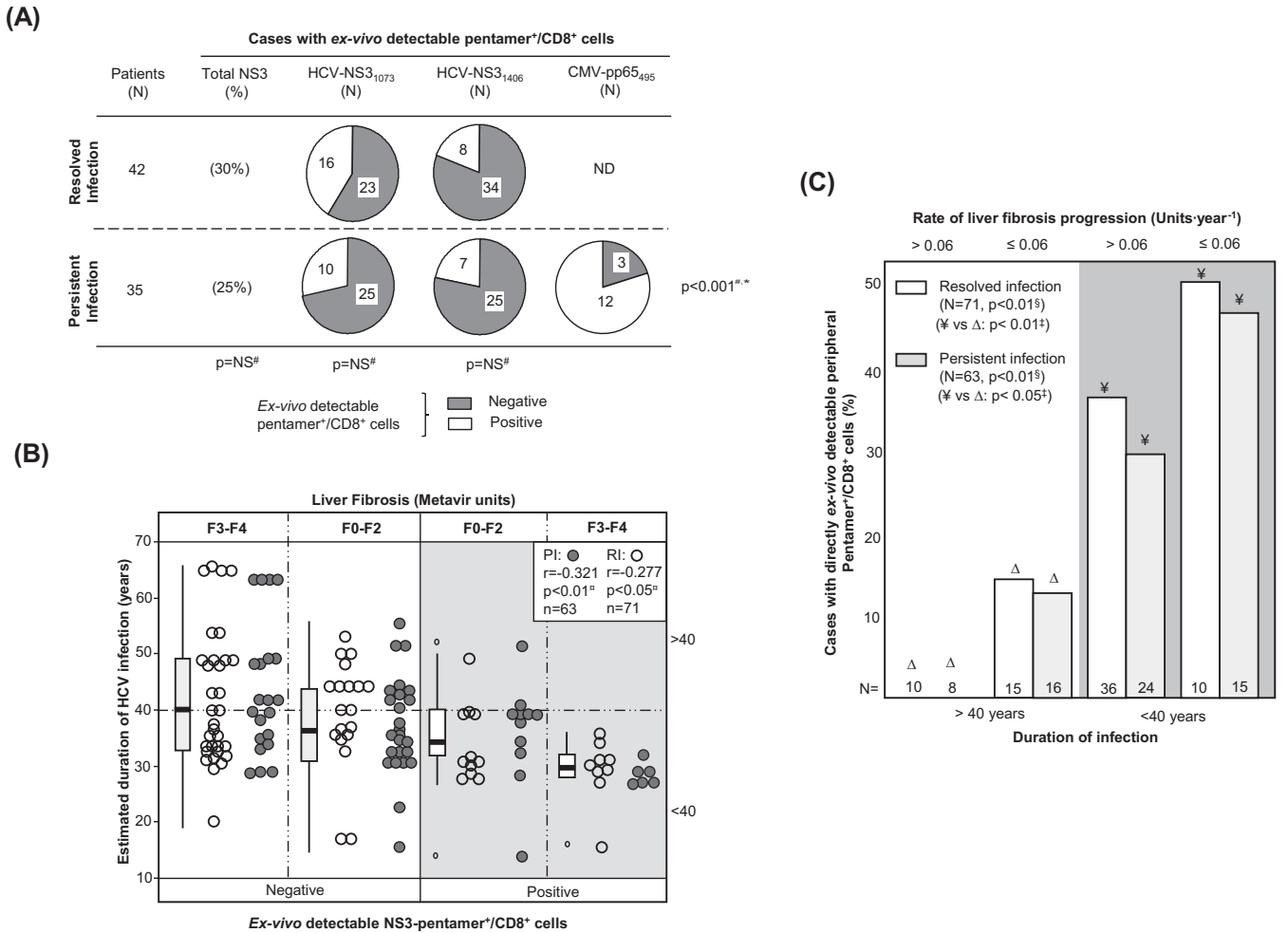
FIG 1 *Ex vivo* detection of pentamer+/CD8+ cells. (A) Frequency of patients with resolved and persistent infections and HCV NS3$_{1073}$-, HCV NS3$_{1406}$-, and CMV pp65$_{495}$-specific pentamer+/CD8+ cells detectable *ex vivo*. (B) Correlation between HCV infection length and detection of peripheral HCV pentamer+/CD8+ cells *ex vivo*, unbundled according to liver fibrosis stage. Box plots represent the distribution of the infection duration in each category when the data for patients with persistent infection and resolved infection after treatment are taken together. (C) Frequency of cases with peripheral pentamer+/CD8+ cells detectable *ex vivo* in relation to the duration of HCV infection (short/midduration, ≤40 years; long lasting, >40 years) and the rate of liver fibrosis progression. #, chi-square test; ¤, Spearman correlation test; ‡, Mann-Whitney U test; §, linear trend test; F, Metavir fibrosis stage; ND, not done; NS, nonsignificant; PI, persistent infection; RI, resolved infection after treatment; *, comparison between HCV-pentamer+/CD8+ and CMV-pentamer+/CD8+ cells in PI.

included for comparisons of patients with PI and RI and also when TRAF1 was the independent variable. In other tests carried out in the PI group, those cases with known HCV escape variants were excluded when TRAF1 was the dependent variable.

The frequency of cases with peripheral HCV-specific pentamer+/CD8+ cells detectable *ex vivo* was similar between the RI and PI groups (Fig. 1A). In patients with PI, cytomegalovirus (CMV) pentamer+/CD8+ cells were more frequently detected than HCV pentamer+/CD8+ cells (Fig. 1A), probably due to persistent antigen stimulation in both pools without exhaustion of the CMV-specific T cell population. Interestingly, the predictive factors associated with the detection of peripheral HCV pentamer+/CD8+ cells were both the duration of HCV infection and the degree of liver fibrosis. A negative correlation between the HCV infection span and the detection of peripheral HCV pentamer+/CD8+ cells was observed in both patients with PI and patients with RI (Fig. 1B; Table 2). In particular, among those patients who had been infected for less than 40 years, pentamer-binding CD8+ cells were observed in 52% of slow fibrosers (liver fibrosis progression rate, ≤0.06 units · year^{-1}) and 32% of mid-rapid-fibrosing cases (liver fibrosis progression rate, >0.06 units · year^{-1}). In contrast, among cases with more than 40 years of disease progression, these cells were detected in only 15% of slow fibrosers and 0% of mid-rapid fibrosers (Fig. 1C).
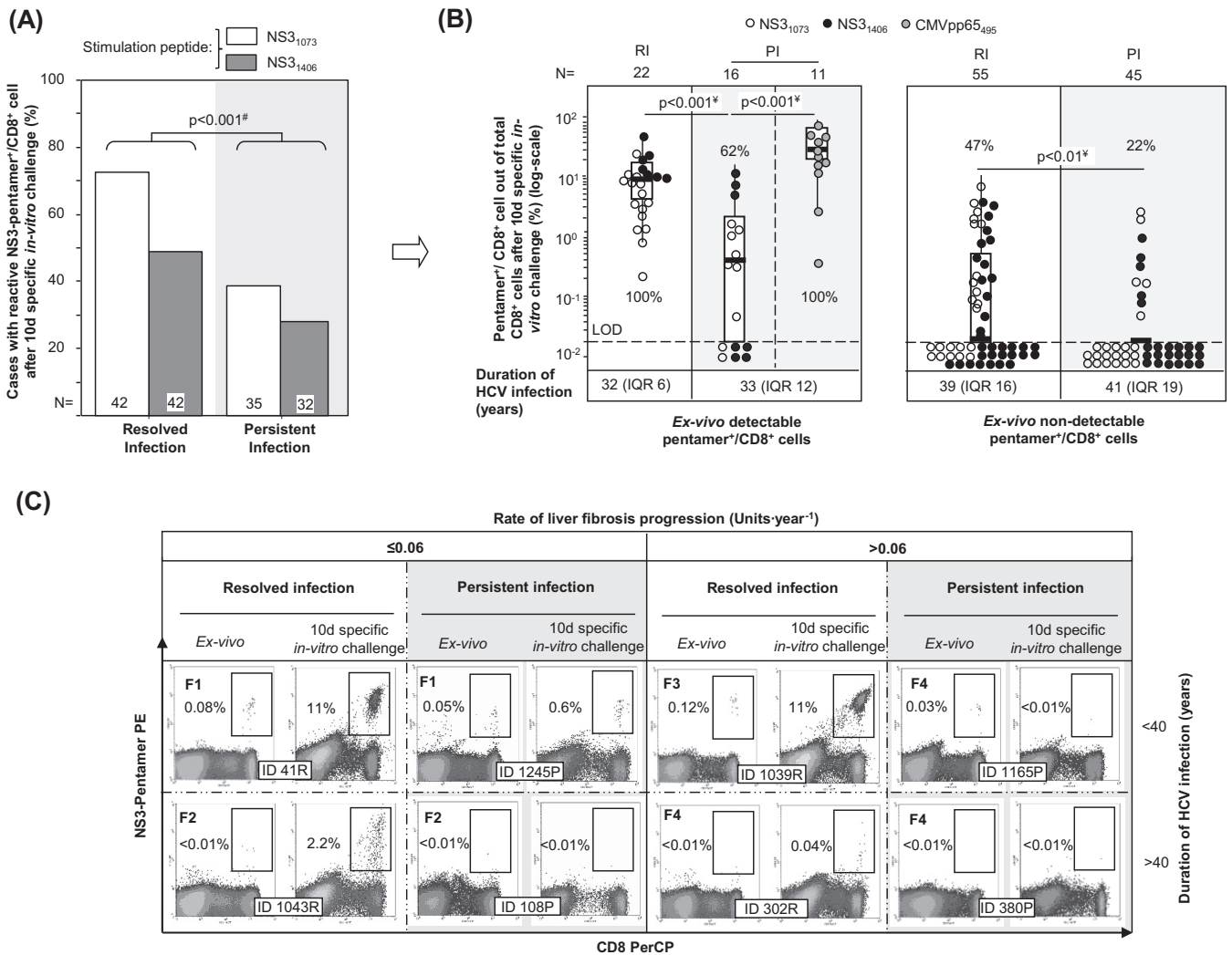
FIG 2 Antigen-specific reactivity of pentamer$^+$/CD8$^+$ cells. (A) Global frequency of cases with pentamer$^+$/CD8$^+$ cell expansion after 10 days (d) of specific stimulation. (B) Intensity of pentamer$^+$/CD8$^+$ cell proliferation in patients with resolved infection (RI) after treatment and persistent infection (PI), according to the presence of pentamer$^+$/CD8$^+$ cells detectable *ex vivo*. The percentages of cases with positive expansion are indicated. The duration of infection (in years) is described as the median plus interquartile range (IQR). Box plots summarize the distribution of pentamer$^+$/CD8$^+$ cell frequency after expansion after pooling of all samples tested in each category. (C) Representative dot plots showing pentamer$^+$/CD8$^+$ cells in the upper right quadrant, according to the duration of infection and the rate of liver fibrosis progression both *ex vivo* and after 10 days of specific *in vitro* challenge. The Metavir score is displayed in bold in the upper left corner. The percentage of pentamer$^+$/CD8$^+$ cells is in reference to the number of total CD8$^+$ cells. d, day; #, chi-square test; ¥, Mann-Whitney U test; ID, patient identification; LOD, limit of detection.

Therefore, the duration of infection and the rate of liver fibrosis progression emerged as key factors determining the presence of detectable peripheral HCV-specific CD8$^+$ T cells by standard pentamer staining.

Impairment of HCV pentamer$^+$/CD8$^+$ cell reactivity during PI. PBL from patients with RI and PI were challenged *in vitro* for 10 days with HCV-specific peptides (NS3$_{1406}$ and NS3$_{1073}$) and in parallel with the CMV pp65 peptide from positions 495 to 504 (pp65$_{495-504}$; also referred to here as the pp65$_{495}$ peptide) as an internal control for patients with PI. In patients with RI, we observed an expansion of 72% of NS3$_{1073}$-specific pentamer$^+$/CD8$^+$ cells and 49% of NS3$_{1406}$-specific pentamer$^+$/CD8$^+$ cells, while only 39% of NS3$_{1073}$-specific pentamer$^+$/CD8$^+$ cells and 27% of NS3$_{1406}$-specific pentamer$^+$/CD8$^+$ cells from the PI group expanded (Fig. 2A). In cases with detectable cells *ex vivo*, 100% of NS3$_{1406}$-specific pentamer$^+$/CD8$^+$ cells and NS3$_{1073}$-specific pentamer$^+$/CD8$^+$ cells from patients with RI proliferated, whereas 77% of NS3$_{1073}$-specific pentamer$^+$/CD8$^+$ cells and 43% of NS3$_{1406}$-specific pentamer$^+$/CD8$^+$ cells

(A)

(B)
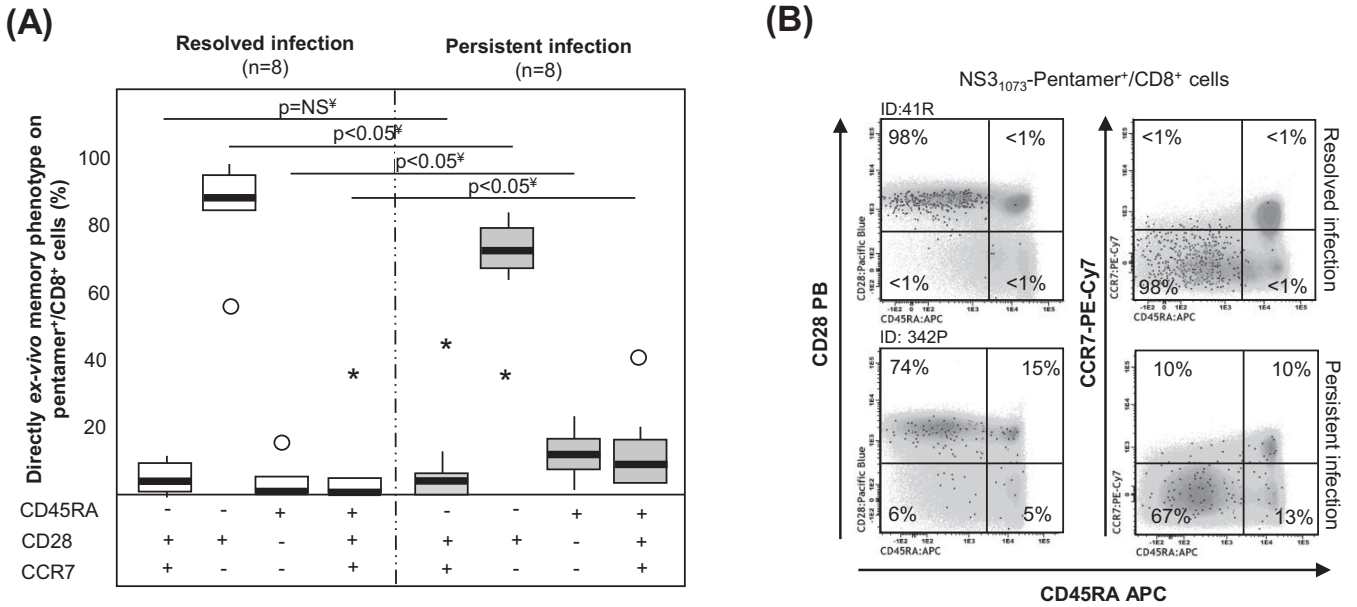
FIG 3 Memory phenotype of pentamer+/CD8+ cells *ex vivo*. (A) Frequency of peripheral central memory effector memory, effector memory RA+ (TEMRA), and naive-like pentamer+/CD8+ cells in cases with resolved and persistent infections. ○, outlier value; *, extreme value. (B) Representative dot plots showing the memory phenotype of pentamer+/CD8+ cells. Black dots, pentamer+/CD8+ cells; gray scale, total CD8+ cells. The data represent the percentage of pentamer+/CD8+ cells in each quadrant in reference to the number of total pentamer+/CD8+ cells. ID, patient identification; ¥, Mann-Whitney U test.

from patients with PI proliferated (Fig. 2B and C). Moreover, after pooling of the data for both epitopes, the intensity of the proliferation, measured as the percentage of pentamer+/CD8+ cells out of the total CD8+ cells, was higher in patients with RI (11.4%) than in patients with PI (0.58%) (Fig. 2B and C). In those cases with no pentamer+/CD8+ cells detectable *ex vivo*, the proliferation was globally lower but still different between the two groups. When the results for the two NS3 epitopes were combined, 47% of pentamer+/CD8+ cells proliferated for the RI group but only 22% proliferated for the PI group (Fig. 2B and C). The proliferation impairment in patients with PI was HCV specific, since 100% of paired CMV pp65$_{495}$ pentamer+/CD8+ cells from those patients expanded after specific *in vitro* challenge (Fig. 2B).

These data showed a weakening of the peripheral HCV-specific CD8+ cell reactivity during chronic infection that was deeper in patients with long-lasting infection, which could suggest the presence of different subsets of target cells according to the duration of HCV infection.

Different HCV pentamer+/CD8+ cell differentiation between PI and RI. In 16 selected samples in which cells were detectable *ex vivo*, we performed an extended analysis of the memory phenotype to describe better the baseline features of specific T cells. In the RI group, >85% of HCV pentamer+/CD8+ cells displayed an effector memory phenotype (CD45RA−, CD28+, CCR7−). In contrast, the patients with PI showed a different memory phenotype distribution, defined by minor subsets of RA-positive (RA+) effector memory T cells (TEMRA; CD45RA+, CD28−, CCR7−) and naive-like cells (CD45RA+, CD28+, CCR7+) and a major pool of CD28-expressing effector memory cells (Fig. 3). The central memory subset (CD45RA−, CD28+, CCR7+) was a minor population in both groups, probably because most of the patients with RI were studied shortly after the sustained viral response. Therefore, a heterogeneous population of peripheral HCV-specific CD8+ T cells but with a significant subset of CD28+ cells, which have previously been considered the source for a positive response to immune modulation, was detected in patients with PI (29).

TRAF1^{low} expression in pentamer+/CD8+ cells after triggering of TCR during PI. A pilot analysis of TRAF1 expression in HCV pentamer-binding CD8+ cells performed directly *ex vivo* showed a slightly higher nonsignificant TRAF1 level in patients with RI

(A)

(B)
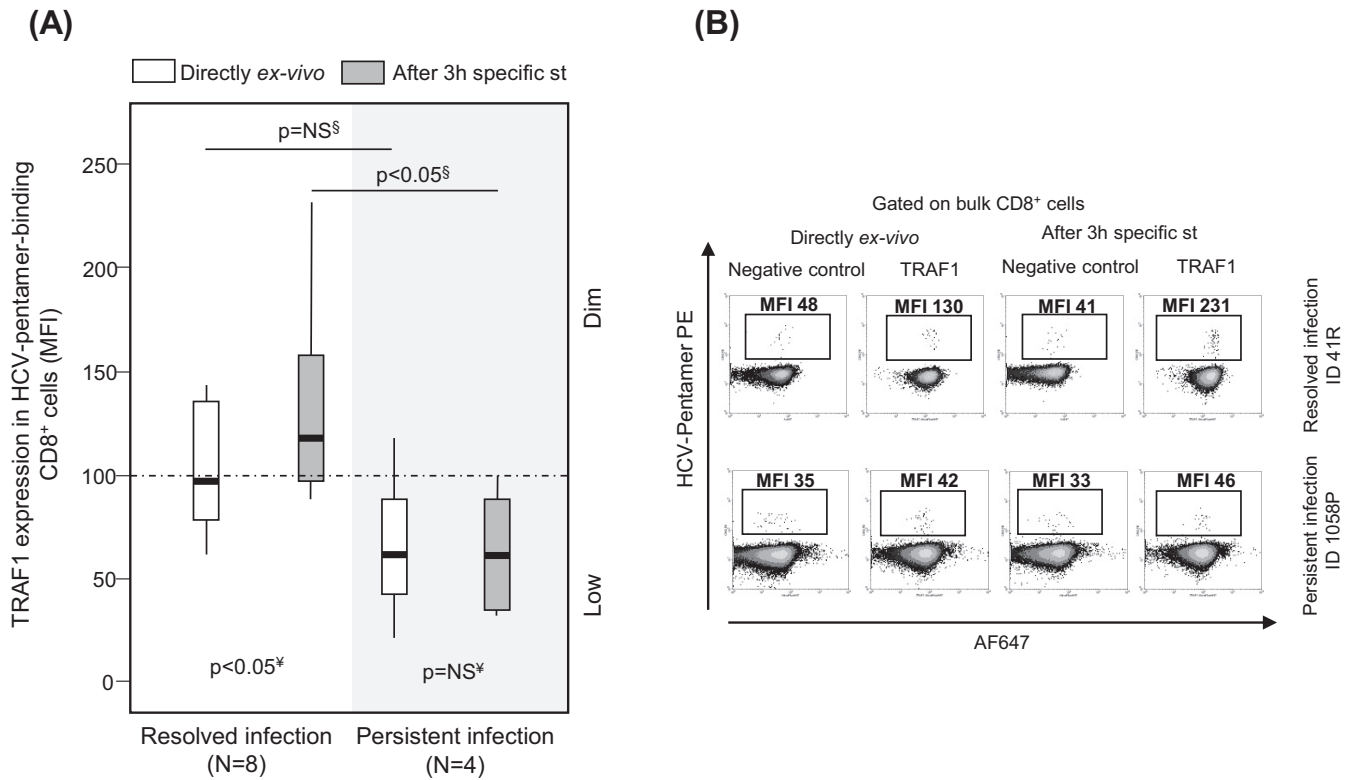
FIG 4 Pilot analysis of TRAF1 expression in pentamer⁺/CD8⁺ cells from patients with resolved and persistent infections performed directly *ex vivo* and after 3 h of specific stimulation. Box plots (A) and representative dot plots (B) from a preliminary analysis show the level of TRAF1 expression in HCV pentamer-binding CD8⁺ cells determined directly *ex vivo* and after 3 h of specific stimulation in patients with a resolved infection after treatment and patients with persistent infection. Negative control, T cell labeling with the secondary antibody only; MFI, mean fluorescence intensity; NS, nonsignificant; st, stimulation; §, Mann-Whitney U test; ¥, Wilcoxon test.

than in patients with PI (Fig. 4). PBL were challenged *in vitro* for 3 h with specific peptides in order to increase the levels of protein expression in both groups, since TRAF1 is an NF-κB-inducible protein with low levels of expression in resting cells (21, 22). TRAF1 was upregulated in patients with RI but not in patients with PI after 3 h of specific triggering of TCR (Fig. 4). According to this strategy and after pooling of the data for the two HCV epitopes tested, the induction of TRAF1 expression in HCV pentamer⁺/CD8⁺ cells after 3 h of specific stimulation was higher in patients with RI (mean fluorescence intensity [MFI], 120; interquartile range [IQR], 70) than in patients with PI (MFI, 80; IQR, 37) (Fig. 5A, C, and D). HCV pentamer⁺/CD8⁺ cells from patients with RI and CMV pentamer⁺/CD8⁺ cells from patients with PI displayed similar levels of TRAF1 induction, both of which were higher than those displayed by HCV penta-mer⁺/CD8⁺ cells from patients with PI (Fig. 5A and C). The level of TRAF1 expression by bulk CD8⁺ cells from patients with RI and PI stimulated with HCV and CMV peptides, respectively, was also higher than that by total CD8⁺ cells from patients with PI stimulated with HCV peptides, although it was significantly lower than that by their paired pentamer⁺/CD8⁺ cells (Fig. 5A and C). This fact could be due to CD8⁺ cell bystander activation during the 3-h PBL-specific stimulation in those cultures with a nonexhausted specific CD8⁺ T cell response to the cognate antigen (30).

According to the level of Alexa Fluor 647 (AF647) MFI expression in the negative controls, three different levels of TRAF1 expression were defined in pentamer⁺/CD8⁺ cells. TRAF1^low expression was considered a value lower than the median for the negative control (34 MFI) plus 1.5 the IQR value, which was 45 (TRAF1^low MFI, ≤100). TRAF1^dim expression was defined as a value lower than 3 times the upper limit of TRAF1^low expression (TRAF1^dim MFI, 100 to 300). TRAF1^high expression was defined as a value higher than the upper limit of TRAF1^dim expression (TRAF1^high MFI, >300).
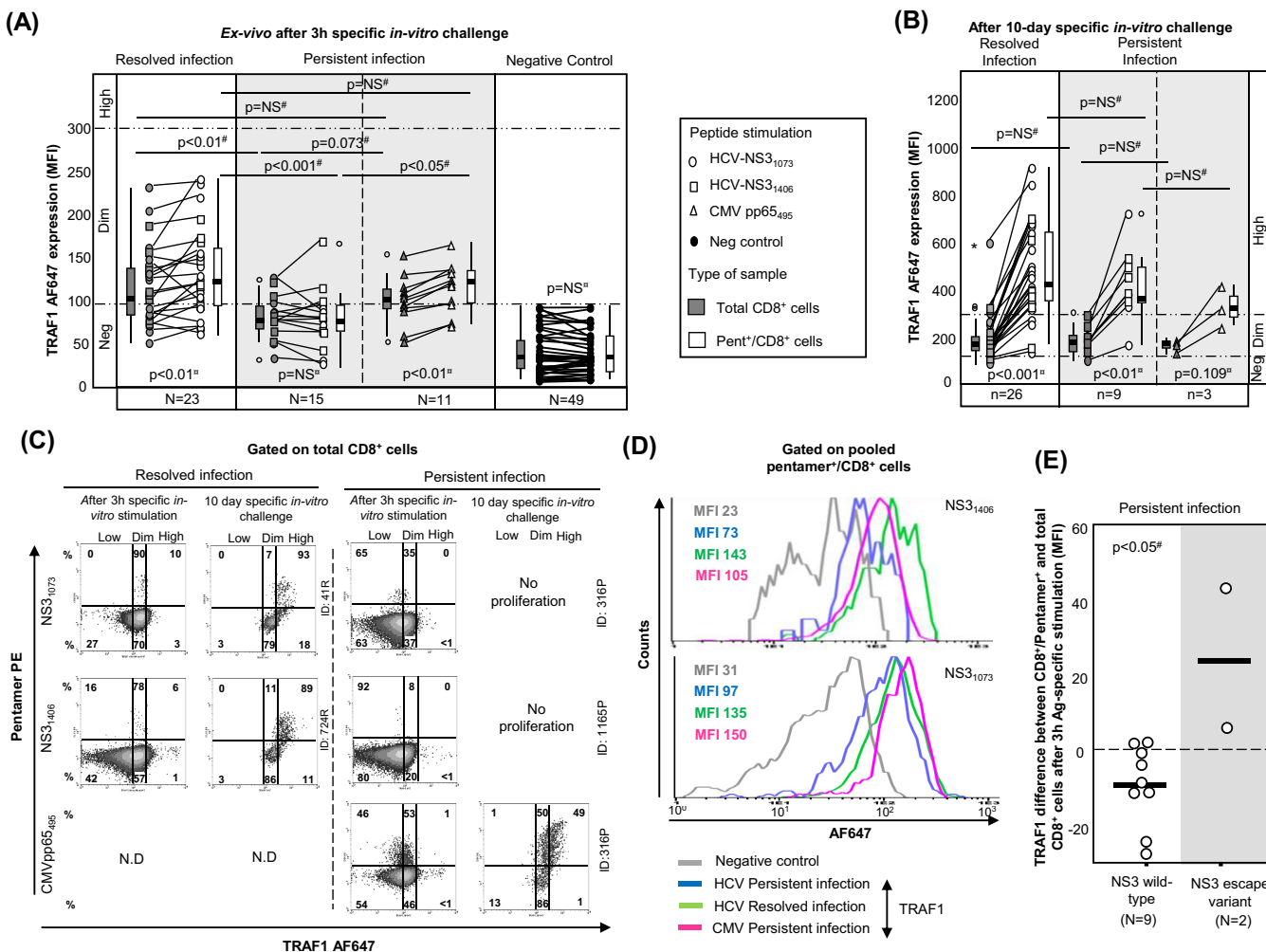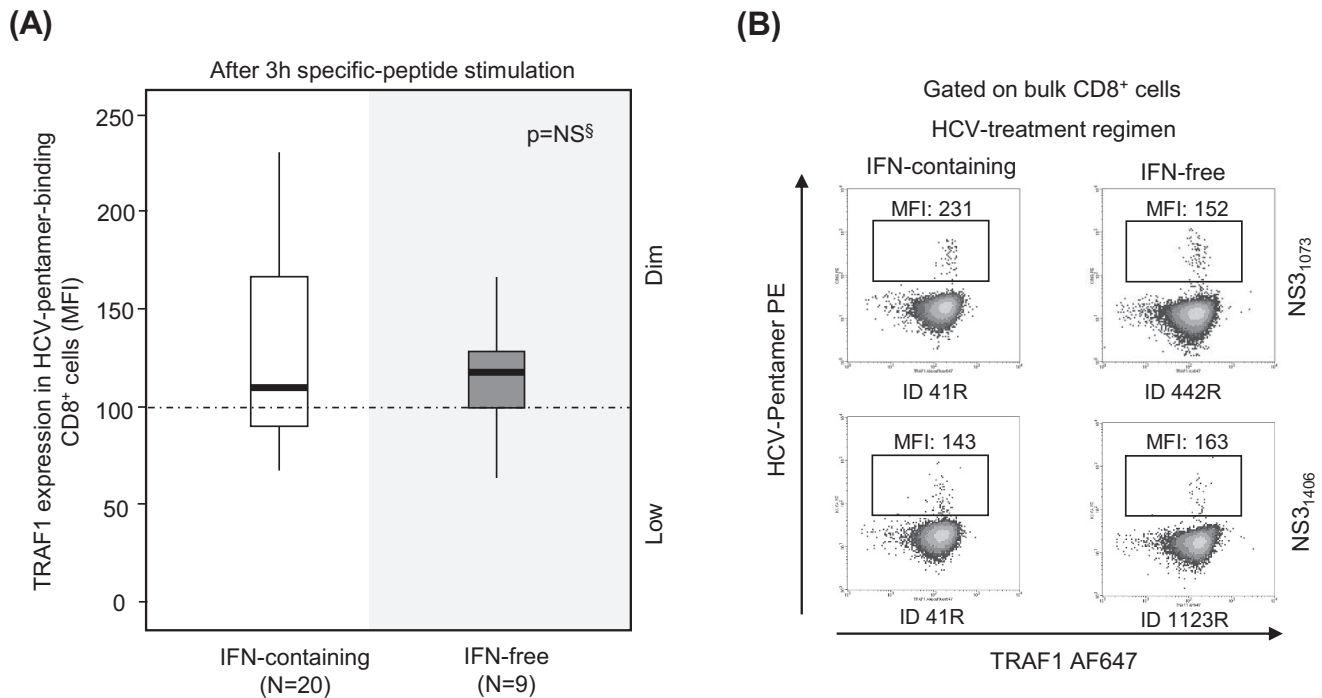
FIG 5 TRAF1 expression in pentamer+/CD8+ cells. (A and B) MFI of TRAF1 in peripheral total CD8+ and pentamer+/CD8+ cells after 3 h (A) and after 10 days (B) of specific *in vitro* challenge, depending on the viral control. According to the MFI, TRAF1 expression was categorized as negative (Neg), dim, and high. The box plots summarize the distribution of the TRAF1 MFI in total and pentamer-binding CD8+ cells in each category. (C) Representative dot plots showing TRAF1 expression in pentamer+/CD8+ cells after 3 h and 10 days of specific *in vitro* challenge in patients with resolved and persistent infections. The data represent the percentage of cells in each area in reference to the number of total CD8+ and pentamer+/CD8+ cells. (D) Histograms of TRAF1 expression by pooled HCV and CMV specific pentamer+/CD8+ cells from all patients with resolved infection and persistent infection after 3 h of specific stimulation. (E) Difference in TRAF1 expression according to the MFI between NS3 pentamer+/CD8+ and total CD8+ cells from patients with PI infected by wild-type HCV NS3 or an escape variant. Bold lines, median values of the distribution; #, Mann-Whitney U test; ¤, Wilcoxon test. ○, outlier value; *, extreme value; Ag, antigen; MFI, mean fluorescence intensity; ND, not done; Negative Control, T cell labeling with the secondary antibody only; NS, nonsignificant; Pent, pentamer.

Using these values as cutoffs, in the RI group, 70% of tested samples showed TRAF1dim expression after 3 h of specific stimulation, while only 20% of samples from the PI group showed TRAF1dim expression (Fig. 5A) ($P = 0.003$). Moreover, in 11 out of 15 patients with PI in whom TRAF1 expression was analyzed, sequencing of the HCV epitope was performed. The difference in the level of TRAF1 induction between pentamer-binding and total CD8+ cells after antigen-specific triggering was lower in samples from wild-type HCV-infected cases than in the two samples harboring escape variants with the already described impaired cross-recognition by wild-type HCV-primed T cells (NS3_{1406}, L1410M) (32) (Fig. 5E).

In 26 patients with RI and 9 patients with PI with a preserved pentamer+/CD8+ cell expansion ability, TRAF1 expression was tested after a 10-day specific *in vitro* challenge. The level of TRAF1 expression was higher than that obtained directly *ex vivo* and higher than that by paired total CD8+ cells (Fig. 5B and C). In fact, in 85% of the experiments with positive pentamer+/CD8+ cell expansion, a TRAF1high phenotype was reached after specific proliferation.

(A)

(B)

FIG 6 TRAF1 expression in pentamer+/CD8+ cells from resolved infection cases after interferon-free and interferon-containing regimens. Box plots (A) and representative dot plots (B) showing the level of TRAF1 expression after 3 h of antigen-specific stimulation in HCV pentamer-binding CD8+ cells from sustained virologic responders to interferon (IFN)-containing and -free regimens. MFI, mean fluorescence intensity; NS, nonsignificant; §, Mann-Whitney U test.

In patients with RI, the induction of TRAF1 expression was comparable in patients treated with interferon (IFN)-free and IFN-containing regimens (Fig. 6). Two patients with PI could be longitudinally studied during anti-HCV treatment with DAA for 12 weeks. In these cases, TRAF1 expression was upregulated in pentamer+/CD8+ cells at the end of treatment and 12 weeks after the cessation of treatment, and this correlated with an improvement in both the frequency of peripheral pentamer-binding CD8+ cells *ex vivo* and the proliferation intensity of pentamer-binding CD8+ cells. After treatment, these cells acquired a PD-1^{dim} CD127^{dim} phenotype, suggesting that they could belong to the T cell factor 1 (TCF)-positive (TCF1+) PD-1+ CD127+ progenitor pool recently described (17) (Fig. 7).

Thus, persistent HCV infection could induce the low level of expression of TRAF1 in peripheral HCV-specific CD8+ T cells; however, in cases in which these cells are not severely exhausted and still maintain their proliferative potential, they are able to acquire a TRAF1^{high} phenotype.

Correlation between TRAF1^{low} expression and exhaustion phenotype. When all cases with HCV pentamer-binding CD8+ cells directly detectable *ex vivo* were taken together, induction of TRAF1 expression in pentamer+/CD8+ cells after 3 h of specific stimulation positively correlated with CD127 and Mcl-1 expression but negatively correlated with PD-1 expression (Fig. 8A and D). After 3 h of specific triggering of TCR, TRAF1^{dim} pentamer+/CD8+ cells showed higher levels of CD127 and Mcl-1 expression but lower levels of PD-1 expression than TRAF1^{low}-expressing cells (Fig. 8B and E). TRAF1^{dim} cells also had a higher intensity of proliferation than TRAF1^{low} pentamer+/CD8+ cells (Fig. 8C and D). Moreover, the percentage of CD107a-positive cells detectable *ex vivo* was higher in the TRAF1^{dim} cell population (41%) than in the TRAF1^{low} cell population (3%) (Fig. 9). In contrast, the level of gamma interferon (IFN-γ) secretion *ex vivo* was similarly low between the TRAF1^{dim} and TRAF1^{low} groups. However, after specific *in vitro* expansion, IFN-γ and CD107a were upregulated in cells of both groups with a preserved expansion ability (Fig. 9). The clinical features of the patients with the TRAF1^{dim} and TRAF1^{low} groups are summarized in Table 3.
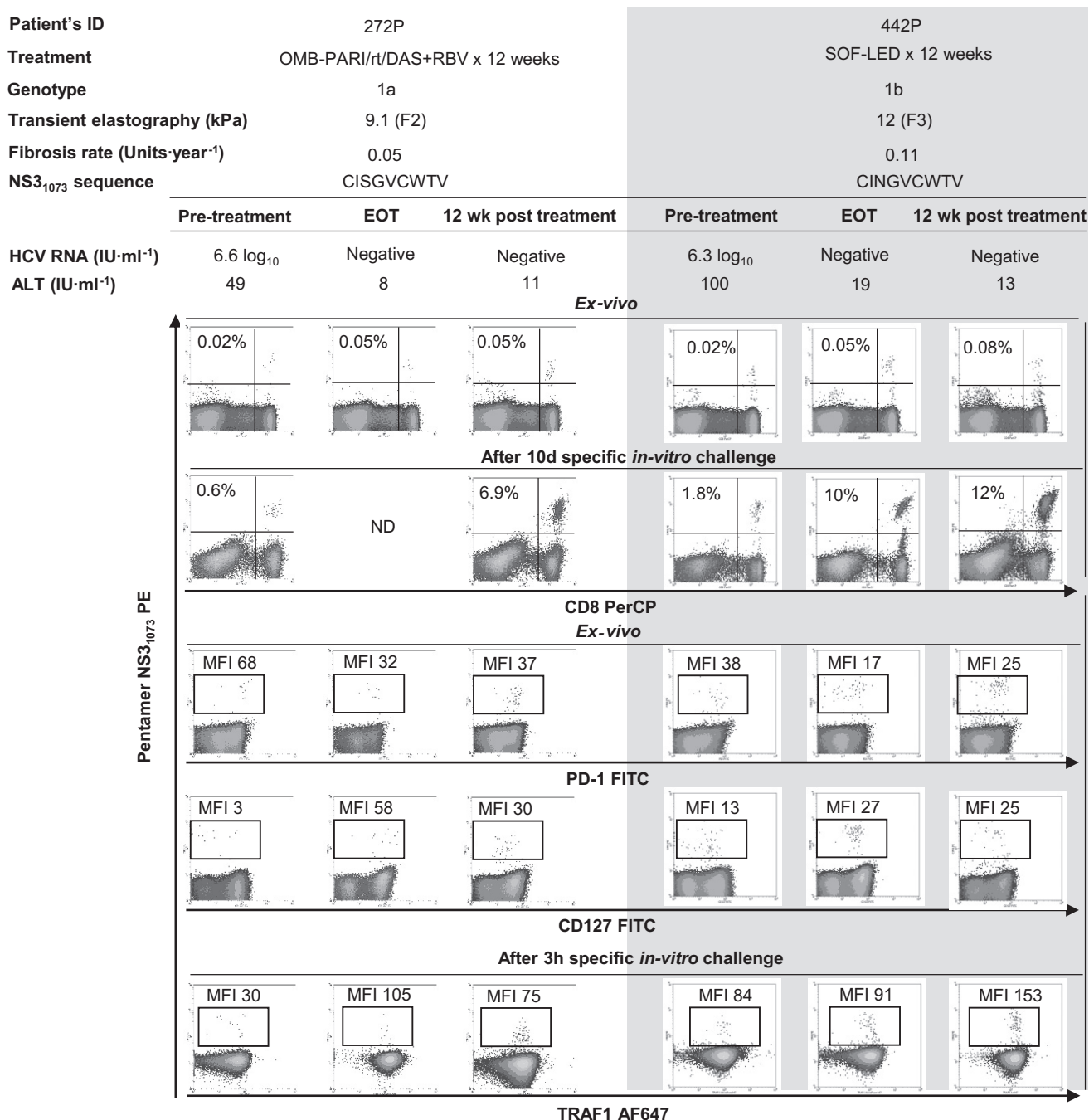
FIG 7 TRAF1 kinetics in pentamer+/CD8+ cells during treatment with direct-acting antivirals. Longitudinal dot plots show the peripheral *ex vivo* frequency, the proliferation intensity after specific *in vitro* challenge, the PD-1/CD127 level obtained directly *ex vivo*, and the level of TRAF1 expression after 3 h of specific stimulation in pentamer+/CD8+ cells from two HCV genotype 1-infected patients during treatment with direct-acting antivirals. ALT, alanine aminotransferase; EOT, end of treatment; OMB-PAR/rt/DAS+RBV, ombitasvir-paritaprevir-ritonavir-dasabuvir plus ribavirin; MFI, mean fluorescence intensity; PBL, peripheral blood lymphocyte; SOF-LED, sofosbuvir plus ledipasvir.

Hence, after specific triggering of the TCR the existence of the TRAF1^low phenotype could point to T cell exhaustion and TRAF1 upregulation could be considered a potential tool to enhance T cell reactivity.

IL-7 upregulates TRAF1 expression, while TGF-β1 does the opposite. After describing a significant positive correlation between IL-7 receptor and TRAF1 expression, we analyzed whether treatment with IL-7 *in vitro* could upregulate TRAF1 expression in pentamer+/CD8+ cells. In 8 out of 9 samples, TRAF1 expression in pentamer+/
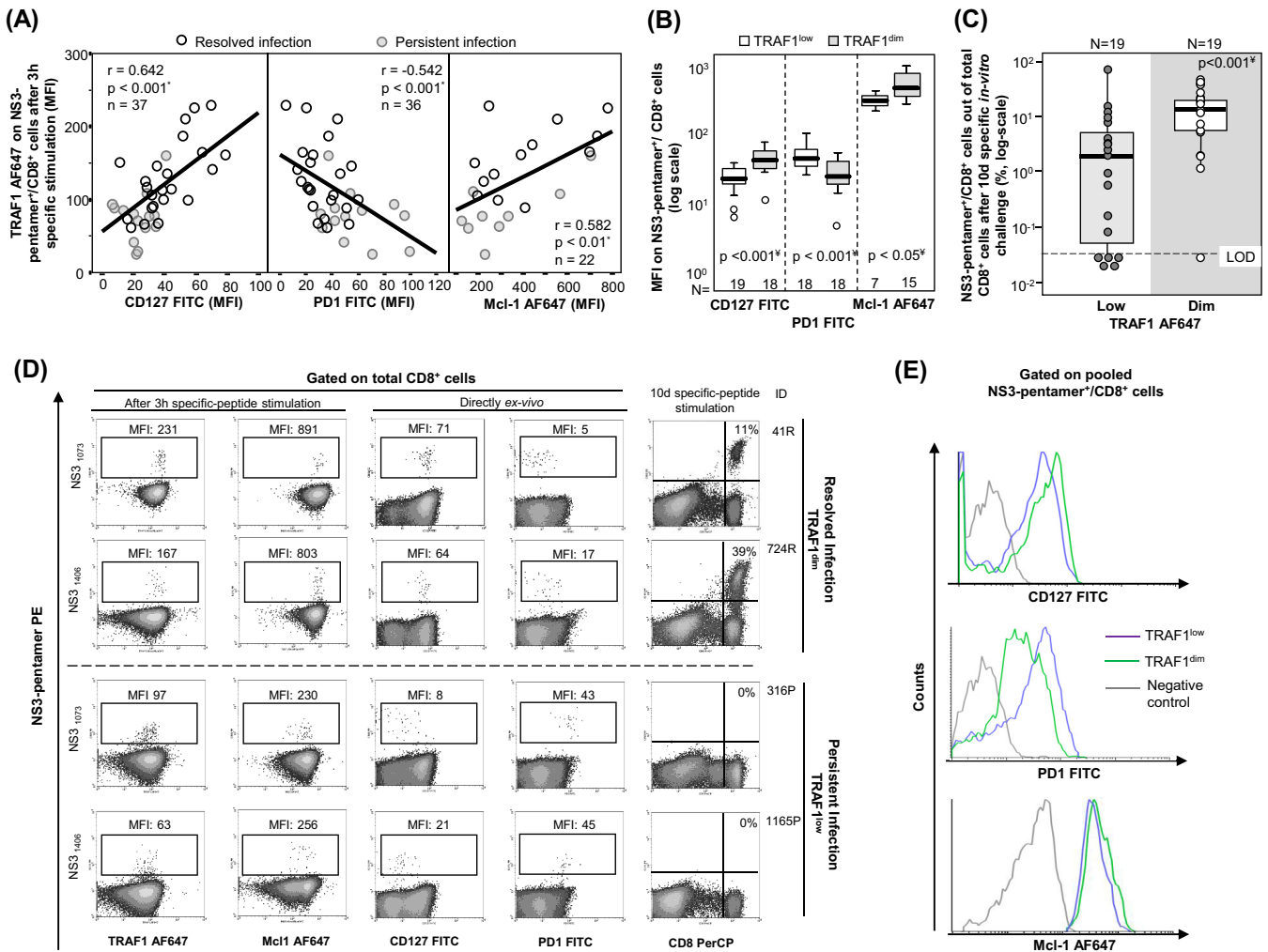
FIG 8 Correlation between TRAF1 expression, exhaustion phenotype, and reactivity of HCV pentamer⁺/CD8⁺ cells. Tests for TRAF1 and Mcl-1 were performed after 3 h of specific peptide stimulation, while PD-1 and CD127 were assessed directly *ex vivo*. (A) Correlation between TRAF1 level and CD127, PD-1, and Mcl-1 expression on pentamer⁺/CD8⁺ cells pooled from patients with persistent and resolved infections. (B) PD-1, CD127, and Mcl-1 expression on HCV pentamer⁺/CD8⁺ cells from HCV patients, according to the TRAF1 level. (C) Rates of HCV pentamer⁺/CD8⁺ cell proliferation after 10 days of specific *in vitro* challenge, depending on the level of TRAF1 expression. (D) Representative dot plots showing the PD-1, CD127, and Mcl-1 phenotype (as the MFI) and the expansion ability (as the percentage of pentamer-binding CD8⁺ cells out of the number of total CD8⁺ cells) according to the TRAF1 level in pentamer⁺/CD8⁺ cells. (E) Histograms of PD-1, CD127, and Mcl-1 expression on pooled pentamer⁺/CD8⁺ cells in relation to the TRAF1 level. *, Spearman correlation test; ¥, Mann-Whitney U test; negative control, T cell labeling with the nonspecific isotype antibody; ○, outlier values; LOD, limit of detection; MFI, mean fluorescence intensity.

CD8⁺ cells was upregulated after 6 days of treatment with IL-7 (20 ng · ml⁻¹) *in vitro* (Fig. 10A and B). Since Bim is upregulated on activated HCV-specific CD8⁺ T cells during chronic infection (9) and is known to be linked to both TGF-β1 secretion (23, 33) and TRAF1 downregulation (34, 35), we also addressed whether TGF-β1 could downmodulate TRAF1 expression in pentamer⁺/CD8⁺ cells. In 7 out of 7 pentamer⁺/CD8⁺ cell assays, TRAF1 expression was downregulated after 48 h of treatment with TGF-β1 (5 ng · ml⁻¹) *in vitro* (Fig. 10A and B).

Interestingly, the culture supernatant of PBL from patients with PI, which achieved a positive expansion after NS3-specific challenge *in vitro*, showed a higher relative decrease in TGF-β1 levels at day 9 that at day 2 of culture than PBL without expansion (Fig. 10C, top). In addition, the absolute negative difference in the supernatant TGF-β1 concentration was higher in samples with positive expansion than in samples without proliferation (Fig. 10C, bottom).

Considering the ability of TGF-β1 to downregulate TRAF1 expression *in vitro* and the fact that the same mechanism could influence the TRAF1 level *in vivo*, we compared the
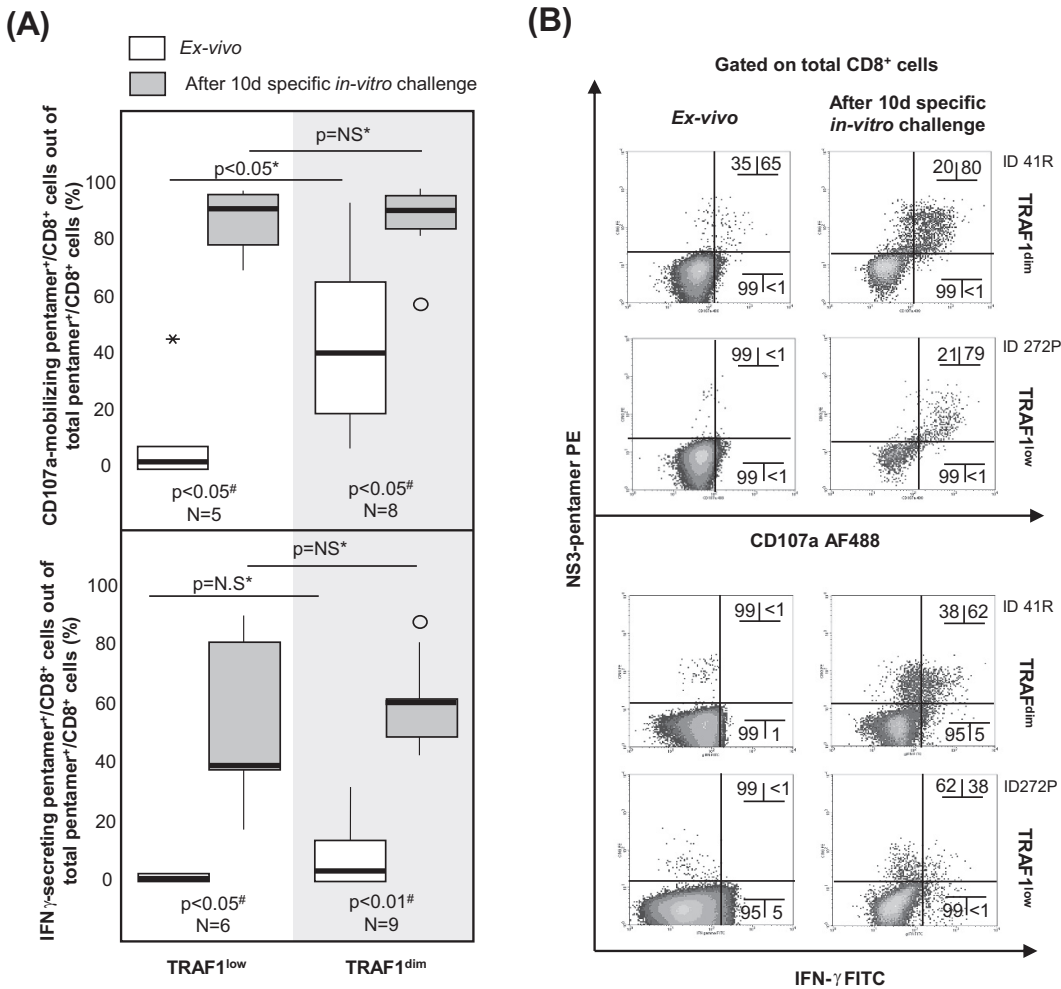
FIG 9 CD107a-mobilizing and gamma interferon (IFN-γ)-secreting HCV pentamer+/CD8+ cells according to the level of TRAF1 expression. Box plots (A) and representative dot plots (B) show the percentage of IFN-γ-secreting and CD107a-mobilizing pentamer+/CD8+ cells *ex vivo* and after 10 days of specific *in vitro* challenge, according to the TRAF1 level, among cells with a preserved expansion ability. ○, outlier value; *, extreme value. The data in each dot plot represent the percentage of positive cells out of the number of either total CD8+ cells or pentamer+/CD8+ cells. NS, nonsignificant; #, Wilcoxon test; *, Mann-Whitney U test.

serum TGF-β1 concentration in patients with RI and those with PI. Serum samples from patients with PI showed a slightly higher TGF-β1 level than those from patients with RI (Fig. 10D, left). This difference translated into a negative correlation between the serum TGF-β1 concentration and TRAF1 induction in HCV pentamer+/CD8+ cells (Fig. 10D, right). Furthermore, we found that TRAF1dim HCV pentamer+/CD8+ cells were associated with lower serum TGF-β1 levels than TRAF1low cells (Fig. 10E).

Our data suggest that IL-7 treatment could be a potential strategy to upregulate TRAF1 by counteracting the TGF-β1-mediated downregulation of TRAF1 in exhausted T cells, in which triggering of TCR alone would not be enough to increase the TRAF1 level.

IL-7 plus 4-1BBL improves HCV pentamer-binding CD8+ cell reactivity. Since a lack of TRAF1 induction in pentamer+/CD8+ cells correlated with impaired reactivity and an exhausted phenotype and because we realized that IL-7 treatment *in vitro* induced TRAF1 upregulation, we analyzed whether IL-7 plus 4-1BBL treatment could improve T cell reactivity in patients with PI. We first performed a pilot study in which we recruited 17 consecutive patients with PI with and without cells detectable *ex vivo* to check if the IL-7 plus 4-1BBL combination could potentially be useful to restore the

TABLE 3 Clinical features of recruited patients with CD8+/pentamer+ cells directly detectable *ex vivo* according to TRAF1 expression[a]

| Characteristic | Value(s) for patients with: | | |
	TRAF1[low] ($n = 19$)	TRAF1[dim] ($n = 19$)	*P* value
% of patients with PI/RI	64/36	15/85	0.003[b]
Median (IQR) age (yr)	53 (11)	57 (10)	NS[c]
% of male patients	68	58	NS[b]
Median (IQR) duration of infection (yr)	34 (11)	32 (5)	NS[c]
Median (IQR) viral load (IU · ml^{-1}, log scale)	5.9 (6.6)	UDL	0.003[c]
Mean (SD) ALT concn (IU · ml^{-1})	64 (76)	35 (9)	0.136[c]
% of patients with significant fibrosis (F3-F4)	57	42	NS[b]
Median (IQR) liver fibrosis progression rate (Metavir score [unit · year^{-1}])	0.074 (0.07)	0.069 (0.06)	NS[c]
% of patients who were slow fibrosers	45	36	NS[b]

[a]ALT, alanine aminotransferase; IQR, interquartile range; NS, nonsignificant; PI, persistent infection; RI, resolved infection after treatment; UDL, under the detection limit.
[b]Determined by the chi-square test.
[c]Determined by the Mann-Whitney U test.

T cell expansion ability. PBL from these cases were challenged *in vitro* with the NS3$_{1406}$ peptide and then received one of the following different treatments: 4-1BBL, IL-7, IL-7 plus 4-1BBL, or β-galactosidase as a negative control. The number of samples with positive expansion increased from 35% in the control group to 65% after IL-7 plus 4-1BBL treatment *in vitro*, while treatment with IL-7 or 4-1BBL alone did not have any significant effect (Fig. 11A).

Subsequently, considering the negative correlation between the duration of HCV infection and the *ex vivo* detection/reactivity of peripheral pentamer+/CD8+ cells, we explored whether IL-7 plus 4-1BBL treatment worked with a similar effectiveness in cases with and without peripheral pentamer+/CD8+ cells detectable *ex vivo*. We analyzed the results of 13 and 39 consecutive proliferation experiments with and without *ex vivo*-detectable pentamer+/CD8+ cells against NS3$_{1406}$ or NS3$_{1073}$ epitopes, respectively. The cases with detectable cells *ex vivo* had an infection length of 31 years, while patients without visible cells had a longer infection span of 40 years (Fig. 11B). Interestingly, in experiments with peripheral cells detectable *ex vivo*, 4-1BBL plus IL-7 treatment increased the proportion of T cell-reactive cases from 61% positive expansion in the control group to 92% positive expansion after the addition of 4-1BBL plus IL-7 treatment (Fig. 11B and E; Table 2). The only nonrestored case was a cirrhotic (degree of liver fibrosis, F4) rapid fibroser patient (patient 1165P) whose T cell reactivity was reestablished by treatment with the combination of 4-1BBL, IL-7, and anti-PD-L1 (Fig. 11E). In cases without detectable cells *ex vivo*, the combination of 4-1BBL plus IL-7 was less effective, only enhancing T cell reactivity in some patients from 20% to 33% (Fig. 11B and E; Table 2).

Treatment with IL-7, 4-1BBL, and anti-PD-L1 improves HCV pentamer-binding CD8+ cell reactivity in slow fibrosers with long-lasting disease. Because of the unsatisfactory restoration of T cell reactivity by using treatment with IL-7 plus 4-1BBL in cases with no pentamer+ cells detectable *ex vivo* and long-lasting disease, we assumed that the exhausted effector memory cell pool could have already disappeared and a potential PD-1-expressing population with stem cell properties but with an impaired regenerative capacity could survive in these cases, as recently suggested (14–16). Therefore, PBL from 20 patients with no pentamer+ cells detectable *ex vivo* were challenged *in vitro* with the combination of IL-7, 4-1BBL, and anti-PD-L1. β-Galactosidase, anti-PD-L1, and IL-7 plus 4-1BBL were used as controls. PBL from 20% of cases expanded after either β-galactosidase or anti-PD-L1 treatment *in vitro*, PBL from 30% of cases proliferated after treatment with the IL-7 plus 4-1BBL combination, and cells from 50% of the cases expanded with treatment with IL-7, 4-1BBL, and anti-PD-L1 (Fig. 11C and E). Globally, the cases with no peripheral pentamer+/CD8+
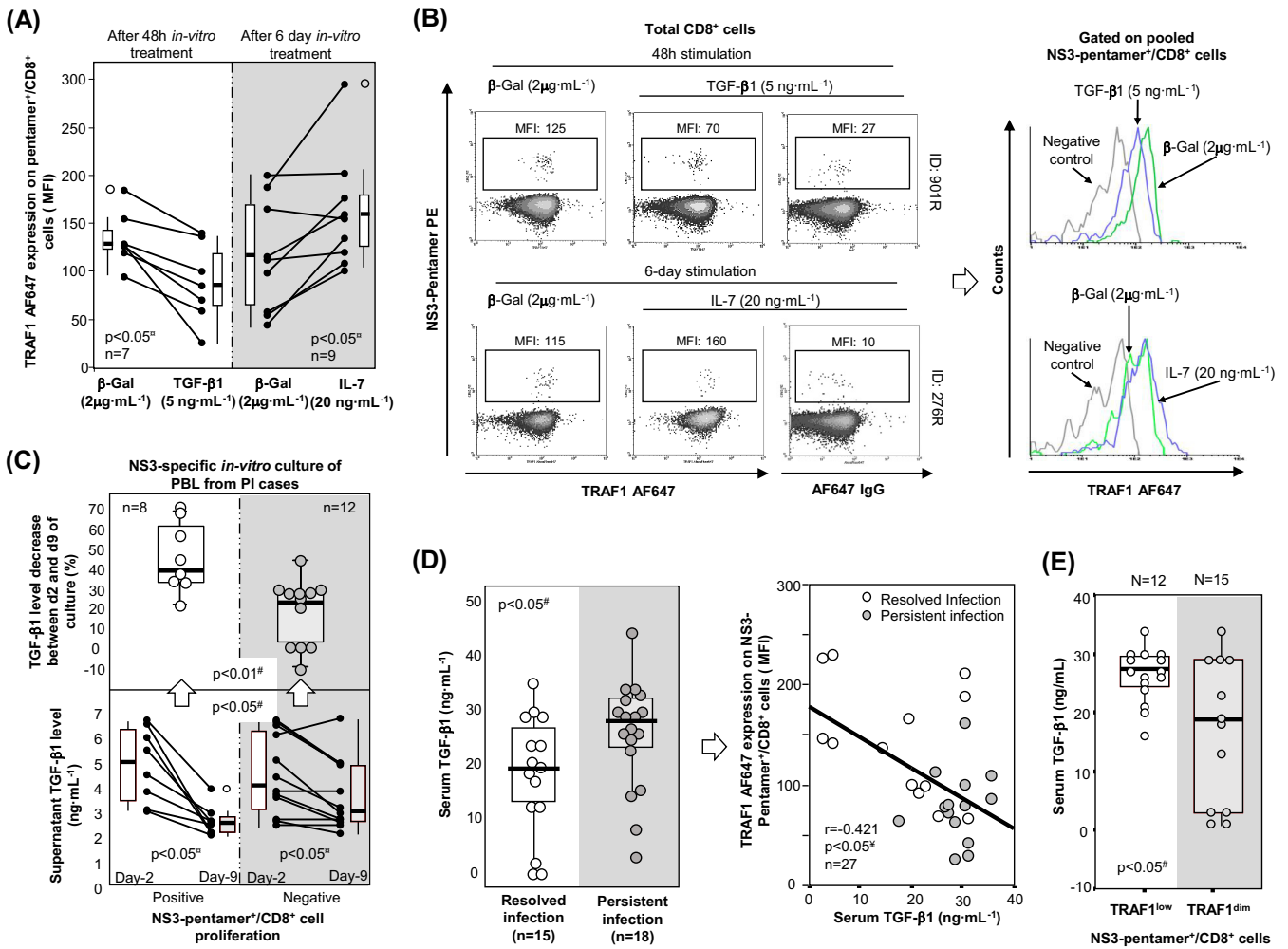
FIG 10 TRAF1 regulation by IL-7 and TGF-β1 in pentamer+/CD8+ cells. (A) Levels of TRAF1 expression in pentamer+/CD8+ cells after β-galactosidase (β-Gal), IL-7, and TGF-β1 treatments *in vitro*. Box plots summarize the distribution of the level of TRAF1 expression in each category. (B) Representative dot plots and histograms showing TRAF1 levels in pentamer+/CD8+ cells after IL-7, TGF-β1, and β-galactosidase treatments *in vitro*. (C) In selected patients with PI, the dynamics of the TGF-β1 levels in PBL culture supernatants between day 2 and day 9 of NS3-specific *in vitro* challenge, according to cell expansion status. (Top) Global variation in TGF-β1 levels; (bottom) individual variation in TGF-β1 levels. Box plots summarize the distribution of either the absolute value or the relative variation in the TGF-β1 level in each category. (D) (Left) Serum TGF-β1 level in patients with persistent infection and resolved infection after treatment. Box plots represent the distribution of the TGF-β1 levels in each group. (Right) Correlation between the serum TGF-β1 level and TRAF1 expression in HCV pentamer+/CD8+ cells after 3 h of specific stimulation. (E) Serum TGF-β1 concentration according to the TRAF1 phenotype of HCV pentamer+/CD8+ cells after 3 h specific stimulation. Box plots summarize the distribution of the TGF-β1 level in every group. ¤, Wilcoxon test; #, Mann-Whitney U test; ¥, Spearman correlation test; ○, outlier value; MFI, mean fluorescence intensity.

cells detectable *ex vivo* that benefited from the combination of IL-7, 4-1BBL, and anti-PD-L1 were patients with low rates of liver fibrosis progression (Fig. 11D and E). Only two cases without cells detectable *ex vivo* and a liver fibrosis progression rate of 0.07 unit · year^{-1} responded to treatment with the combination of IL-7, 4-1BBL, and anti-PD-L1, but these two cases had short/midduration infections of 29 years (Fig. 11D and E).

Hence, our data suggest that IL-7 plus 4-1BBL treatment could improve HCV-specific cytotoxic T cell reactivity in patients with short/midduration infections. However, in cases with disease for longer durations, a more severe T cell exhaustion is usually present, making an additional blockade of the PD-1/PD-L1 checkpoint necessary to enhance the T cell proliferative potential.

DISCUSSION

In order to establish a persistent infection, HCV induces the exhaustion or even deletion of the HCV-specific CD8+ T cell response (8, 10). Among other strategies, HCV
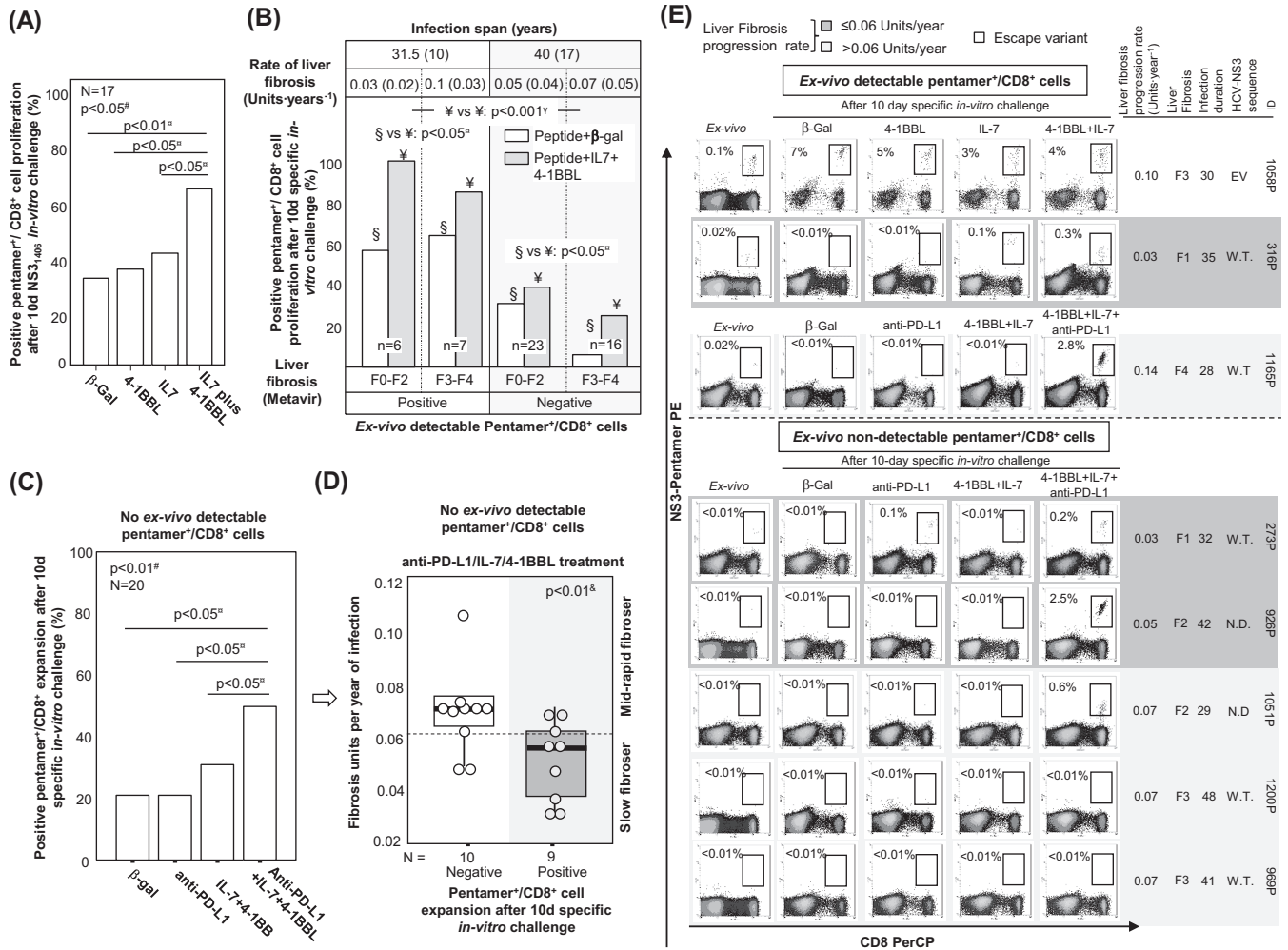
FIG 11 Restoration of pentamer+/CD8+ cell reactivity. (A) In patients with persistent infection, the percentage of assays with pentamer+/CD8+ cell expansion after 10 days of NS3$_{1406}$ challenge in vitro in the presence of treatment with β-galactosidase (β-gal), IL-7, 4-1BBL, or IL-7 plus 4-1BBL. (B) Cases with pentamer+/CD8+ cell proliferation after antigen-specific stimulation in the presence of treatment with β-galactosidase or IL-7 plus 4-1BBL, according to the detection of peripheral pentamer+/CD8+ cells ex vivo. The rate of liver fibrosis progression and the duration of infection are expressed as the median plus interquartile range. Liver fibrosis is described by the Metavir score. (C) Percentage of cases without cells detectable ex vivo with pentamer+/CD8+ cell proliferation after treatment with β-galactosidase, anti-PD-L1, IL-7 plus 4-1BBL, or IL-7, 4-1BBL, and anti-PD-L1. (D) In patients with PI without cells detectable ex vivo, the liver fibrosis progression rate according to the proliferative potential after specific in vitro treatment with IL-7, 4-1BBL, and anti-PDL1. Box plots summarize the distribution of the liver fibrosis progression rate in each group. In the group positive for expansion, one case was not included because the estimated date of infection was unknown. (E) Representative dot plots showing the expansion of CD8+/pentamer+ cells in the presence of different treatment combinations, according to the detection of CD8+/pentamer+ cells ex vivo and the liver fibrosis progression rate. The data in each dot plot show the frequency of pentamer+/CD8+ cells out of the number of total CD8+ cells. EV, escape variant; F, Metavir fibrosis score; N.D., not done; ○, outlier; W.T., wild type; #, Friedman test; γ, chi-square test; ¤, Wilcoxon test; &, Mann-Whitney U test.

modulates T cell costimulatory pathways for this purpose (36). An understanding of these pathways could lead to the development of new therapies focused on the restoration of these impaired checkpoints (37). 4-1BB/4-1BBL is a costimulatory checkpoint that has been involved both in effector capabilities and in inhibition of the Bim-regulated apoptosis of virus-specific cytotoxic T cells during influenza virus and human immunodeficiency virus (HIV) infections (34, 35). However, this pathway can become dysfunctional due to the virus-induced loss of its key signal transducer (TRAF1) (23). Although the triggering of 4-1BB/4-1BBL could be a promising target for improving T cell reactivity during HCV infection, this strategy has not been effective in restoring intrahepatic HCV-specific CD8+ T cells (13), further adding to the potential role of TRAF1 downregulation (23).

In view of this, we designed a cross-sectional study to understand the role of the 4-1BB/TRAF1 checkpoint with the purpose of exploring a potential in vitro therapy to

enhance HCV-specific CD8$^+$ T cell reactivity. We compared the specific T cell response between patients with RI after treatment and patients with PI. We selected responders to anti-HCV treatment as the positive controls, since reactive HCV-specific CD8$^+$ T cell detection after treatment correlates with a sustained viral response in IFN-based and -free treatments (2, 3, 17), probably by T cell control of temporary occult traces of HCV (4–7). In addition, CMV-specific CD8$^+$ T cell responses were also assessed in patients with PI as an internal positive control due to the ability of these cells to naturally restrain a persistent viral infection. We chose two HLA-A2 immunodominant NS3 epitopes (NS3$_{1406}$ and NS3$_{1073}$) with a low frequency of escape variants as the model for our study (38, 39). We performed epitope sequencing in a few patients with PI to address the rate of escape variants in our cohort. One hundred percent of the samples with NS3$_{1073}$ and 70% of the samples with NS3$_{1406}$ tested were wild type or had conservative amino acid substitutions (32, 40). Therefore, the results obtained with our cohort allowed us to draw conclusions about the influence of HCV pressure on TRAF1 expression.

First, we assessed the basic functional and phenotypic features of HCV-specific CD8$^+$ cells in the recruited cases. We observed that the chance of detecting *ex vivo* peripheral pentamer$^+$/CD8$^+$ cells was similar between patients with RI and patients with PI, although this was probably due to different causes; the lack of sustained priming in patients with RI and the overwhelming persistent antigen stimulation during PI could impact the peripheral detection of HCV-specific CD8$^+$ T cells, as suggested by mathematical models (41). The only factor predictive of T cell detection was the duration of infection in combination with the speed of liver fibrosis development. We calculated the rate of liver fibrosis progression based on the estimated date of infection and the result of one liver biopsy or liver transient elastography at the time of recruitment into the study or the date of cirrhosis diagnosis, based on clinical records. This approach has been shown to be valid, since Poynard et al. found that the estimated rate of liver fibrosis progression per year, based on one liver biopsy sample from patients for whom the duration of infection was known, was similar to the rates of progression estimated from paired biopsy samples (42).

In our study, the longer that the duration infection was and the higher that the rate of liver fibrosis progression was, the lower was the likelihood that HCV-specific CD8$^+$ effector cells would be detected. This finding could mean that in long-lasting infection, the HCV-specific CD8$^+$ effector cells could both be more prone to apoptosis and not be replenished due to a severely impaired progenitor pool (15, 16). The misbalance between proapoptotic proteins (8) and antiapoptotic proteins (9, 17) could lead to the progressive deletion of the effector memory cell pool over the years, like that which occurs with LCMV-specific CD8$^+$ cells during chronic infection (31). Finally, after the loss of these effector cells, the progression of liver fibrosis could advance faster.

To better define the baseline features of the studied cells, we carried out a more sensitive analysis of the memory cell subpopulations in our cohort (43, 44). A homogeneous effector memory phenotype was observed in patients with RI, while patients with PI had minor populations of TEMRA and naive-like T cells but also a major group of CD28$^+$ PD-1-expressing effector memory cells that could theoretically be sensitive to a PD-1 blockade (29). We could also speculate that PD-1 could affect not only the positive checkpoint CD28 (45) but also other positive costimulatory pathways, such as the 4-1BB/TRAF1 pathway, in a similar manner. In fact, we observed in our study a negative correlation between PD-1 expression and TRAF1 expression.

In patients with PI, the reactivity of CD8$^+$ T cells was clearly reduced for HCV-specific CD8$^+$ cells but not for paired CMV-specific CD8$^+$ cells, as predicted by mathematical models (41). In line with the reduced peripheral T cell detection, this HCV-specific hyporeactivity was stronger in long-lasting disease. This could be due to different levels of exhaustion of the targeted T cells according to the duration of HCV infection. The population keeping a proliferative potential during a chronic viral infection seems to be either a stem cell-like subset with a PD-1^{dim} T-bet^{high} phenotype (16) or a memory-like pool characterized by the phenotype TCF1$^+$ PD-1$^+$ CD127$^+$ T-bet^{dim} eomesodermin^{low}

(Eomes^{low}) (15, 17). They are mainly found in the lymphoid tissues (15) but can be also detected in the peripheral compartment during chronic HCV infection and after treatment-induced resolved HCV infection (16, 17). Although these populations could be contracted during PI, it is possible that they could still be targeted by immunotherapeutic approaches, such as PD-L1 blockade or IL-7 stimulation, since they expressed the respective receptors. Nevertheless, the immunomodulation needs of these cells could be different depending on the infection stage.

After we described the basic features of the peripheral HCV-specific CD8$^+$ T cells according to viral control and the duration of infection, we analyzed whether the 4-1BB/TRAF1 pathway could be involved in the observed progressive impairment of T cell reactivity in the course of the natural history of the PI. The level of antigen-specific TRAF1 expression induced in HCV-specific CD8$^+$ T cells was higher in patients with RI than in patients with PI. In all the experiments with positive expansion, the TRAF1 phenotype was TRAF1^{high} after proliferation, suggesting that TRAF1 could play a role in T cell reactivity. We also detected a slightly higher TRAF1 level in bulk CD8$^+$ cells from patients with RI and PI after specific stimulation with HCV and CMV peptides, respectively, than in patients with PI stimulated with HCV antigens. This finding could be explained by the occurrence of bystander CD8$^+$ cell activation in cultures with specific T cells reactive to the cognate antigen (30). Besides the cross-sectional difference in TRAF1 induction between patients with RI and patients with PI, the role of HCV pressure on TRAF1 inducibility in HCV-specific CD8$^+$ T cells was also confirmed by the higher level of TRAF1 expression in patients with PI harboring HCV escape variants (32) and by the upregulation of TRAF1 after anti-HCV treatment in patients with PI reaching a sustained viral response.

In addition to determining a low level of TRAF1 in HCV-specific CD8$^+$ T cells during chronic HCV infection, we also found that the TRAF1^{low} phenotype correlated with impaired reactivity and an exhausted phenotype. TRAF1^{low} cells had a lower proliferative potential and lower levels of CD107a mobilization after the antigen-specific triggering of TCR than TRAF1^{dim} cells, as well as an exhausted and proapoptotic phenotype (CD127^{low}, PD-1^{high}, Mcl-1^{low}). It is possible that the low Mcl-1 level in TRAF1^{low} cells could not counteract the Bim upregulation that occurs after an antigen encounter during chronic HCV infection (9). The loss of TRAF1 has been described to lead to Bim upregulation in a murine model of influenza virus infection (35). Consequently, the TRAF1^{low} phenotype could be associated with a Bim/Mcl-1 misbalance that induces T cell apoptosis. The triggering of 4-1BB has been shown to restore this balance, reestablishing T cell reactivity through Bim downregulation (34). To make this pathway operative in patients with chronic HCV infection, it would be necessary to restore its fundamental signal transducer (TRAF1). To achieve this goal, we tested the effects of two regulatory cytokines with modulatory properties on TRAF1 in LCMV infection (23). We demonstrated that IL-7 significantly increased the level of TRAF1 expression in HCV-specific CD8$^+$ cells, while TGF-β1 had the opposite effect. Moreover, in vitro cultures of cells from patients with PI with positive HCV-specific CD8$^+$ cell proliferation showed a consistent decrease in the TGF-β1 level that was lower in most cases of nonexpanding cells. This difference could be explained by the IFN-γ secretion by reactive HCV-specific CD8$^+$ cells observed after proliferation in our cohort, since IFN-γ is able to inhibit the differentiation of T cells into inducible TGF-β1-secreting T regulatory cells (iTreg) (46). All these data suggested that TGF-β1 could affect T cell activation through TRAF1 downregulation. This situation might also occur in vivo, and in fact, we found a slightly higher TGF-β1 level in serum from patients with PI than in serum from patients with RI. This translated into a negative correlation between the TGF-β1 concentration and the induction of TRAF1 expression after specific stimulation in peripheral HCV-specific CD8$^+$ cells. Previous studies have also shown that HCV-specific CD8$^+$ cells from patients with chronic HCV infection are able to secrete TGF-β1 after the specific triggering of TCR (24), that HCV itself is able to induce TGF-β1 expression by liver cells (25, 26), and that the levels of TGF-β1-secreting Treg could be increased during PI (47), all of which could contribute to TRAF1 downregulation.

However, the effect of TGF-β1 *ex vivo* is likely most relevant in exhausted T cells, in which the lack of TRAF1 upregulation after the triggering of TCR (22) could not overcome the TGF-β1-induced loss of TRAF1. In fact, in reactive CMV-specific CD8 T cells from cases with PI, the TRAF1 levels after specific *in vitro* challenge were similar to those in HCV-specific cells from patients with RI, despite the different serum TGF-β1 level.

Once we observed that treatment with IL-7 *in vitro* could upregulate TRAF1 expression, we hypothesized that stimulation with IL-7 plus 4-1BB could enhance HCV-specific CD8+ T cell reactivity. Although during chronic hepatitis C the IL-7 receptor is down-regulated in intrahepatic HCV-specific CD8+ T cells (8), a peripheral pool of CD127^{dim} cells can still be detected (8, 17), and consequently, this subset could respond to our therapy. Our data showed a significant global improvement in the number of reactive patients with PI after treatment with IL-7 plus 4-1BBL but not after treatment with either IL-7 or 4-1BBL alone. Therefore, the reported failure of 4-1BBL to improve the intrahepatic HCV-specific cytotoxic response (13) could be due to the lack of the key signal transducer of this checkpoint (TRAF1). Nevertheless, the treatment with IL-7 plus 4-1BBL was completely active only in patients with short/middduration infections, characterized by HCV-specific CD8+ cells detectable *ex vivo*, while in cases without visible cells and long-lasting disease, the treatment was less effective.

Based on the previous reports of peripheral stem cell-like subsets (16) and progenitor memory-like subsets (17) expressing PD-1 during chronic viral infections, we tested whether PD-1 blockade, in addition to 4-1BB stimulation after IL-7-mediated TRAF1 upregulation, could restore T cell reactivity in these more advanced cases. IL-7 treatment alone during the initial effector phase can prevent T cell exhaustion (27), but later, exhausted T cells respond poorly to IL-7 (48). Interestingly, anti-PD-L1 could improve IL-7 receptor signaling and could again make exhausted virus-specific CD8+ cells sensitive to the effect of IL-7 (49). We found that treatment with anti-PD-L1, IL-7, and 4-1BBL *in vitro* restored the reactivity of HCV-specific CD8+ cells in a significant proportion of those cases without pentamer+/CD8+ cells detectable *ex vivo*.

To better define this response, we looked for predictive factors associated with the recovery of T cell reactivity in these cases. The responder patients were those with a low rate of liver fibrosis progression. Supporting our finding, it has been reported that TGF-β1 blockade restores the HCV-specific cytotoxic T cell effector response in slow fibrosers but not in rapid fibrosers (50). According to our data, this improvement could be linked to TRAF1 upregulation as a consequence of either TGF-β1 blockade, as in the previously described study (50), or IL-7 stimulation, as in our work.

In difficult-to-treat HCV cases with advanced disease, the potential lack of restoration of a specific T cell response after treatment could also be one of the causes of failure of treatment with DAA, due to the inability to control minor viral traces resistant to treatment, favoring subsequent viral relapse (3–5, 51). In these cases, additional immunomodulatory treatments, like the one proposed in this paper, could be an interesting add-on strategy to increase the efficacy of DAA.

To sum up, our data support novel ways of restoring T cell responses in patients with chronic HCV infection, stressing the key role of TRAF1 signaling, which could be a promising target for immunotherapy in patients with chronic viral infections and tumors. IL-7-induced TRAF1 upregulation could be a useful strategy in cases with still detectable exhausted peripheral effector memory cells. Nevertheless, in our cohort, patients without detectable HCV-specific cells maintained a target population that could be expanded by additional blockade of the negative checkpoint, PD-1/PD-L1.

MATERIAL AND METHODS

Patients. Seventy-seven human leukocyte antigen (HLA)-A2-positive HCV genotype 1-positive patients with PI ($n = 35$) and resolved infection (RI) after treatment ($n = 42$) were recruited at the Guadalajara University Hospital, Guadalajara, Spain. Patients with human immunodeficiency virus (HIV) coinfection, any other concurrent liver disease, risk factors for liver steatosis, or levels of alcohol consumption greater than 40 g per day were excluded. Heparinized peripheral blood (60 ml) and a serum

sample were withdrawn at recruitment. The samples from cases with RI were taken at least 12 weeks after the end of treatment. In two patients with PI subjected to DAA treatment, peripheral blood samples were also withdrawn before, at the end of, and 12 weeks after treatment. The duration of infection was estimated according to the moment of exposure to the HCV risk factor (52). The time point for the diagnosis of liver cirrhosis was defined by either clinical/analytical data or the estimation of fibrosis through liver stiffness or biopsy, obtained from the patients' clinical records. A liver transient elastography with a FibroScan-402 device (Echosens, France) or a liver biopsy was carried out at the time of enrollment. The speed of liver fibrosis progression was calculated by the ratio between liver fibrosis score and either the estimated duration of infection or the time gap until the diagnosis of cirrhosis. Fibrosis was categorized according to the Metavir score (53). An individual with a fibrosis progression rate of ≤ 0.06 units $\cdot$ year^{-1} was considered a slow fibroser, while one with a rate higher than 0.06 units $\cdot$ year^{-1} was categorized as a mid/rapid fibroser (42). The Research Ethical Committee of the Guadalajara University Hospital (Guadalajara, Spain) approved the study protocol, which conformed to the ethical guidelines of the 1975 Declaration of Helsinki. All the patients enrolled in the study gave written informed consent. Table 1 summarizes the clinical features of the study groups.

Synthetic peptides and pentamers. HLA-A2-restricted peptides corresponding to the HCV genotype 1 NS3 region from positions 1406 to 1415 (NS3$_{1406-1415}$; KLVALGINAV), NS3$_{1073-1081}$ (CINGVCWTV), cytomegalovirus (CMV) pp65$_{495-504}$ (NLVPMVATV), and phycoerythrin (PE)-conjugated HLA-A2/peptide pentameric complexes (pentamer) loaded with the same NS3 and CMV peptides were purchased from ProImmune (Oxford, UK). These HCV pentamers allow the detection of CD8$^+$ cells specific for the epitopes NS3$_{1073}$ of HCV genotypes 1a (CINGVCWTV) and 1b (CVNGVCWTV) and NS3$_{1406}$ of genotype 1a (KLVALGINAV and KLVALGVNAV) (40).

Virological assessment and tissue typing. Screening for the HLA-A2 haplotype, anti-HCV, HCV genotype, HCV RNA load, and HCV-NS3$_{1406-1415}$ and NS3$_{1073-1081}$ epitope sequences was performed as previously reported (8). The consensus sequences and sequences with conservative amino acid changes within the consensus sequence were considered the wild-type sequence. A test for CMV IgG status was carried out for patients with PI by use of the Architect CMV IgG assay (Abbott Laboratories, Ireland).

Antibodies. The following mouse anti-human monoclonal antibodies (MAb) were used for flow cytometry: anti-CD8-peridinin chlorophyll (PerCP) (clone SK1; BioLegend, San Diego, CA), anti-CD8-allophycocyanin (APC)-H7 (clone SK1; Becton Dickinson Bioscience, San Jose, CA), anti-CD127-fluorescein isothiocyanate (FITC) (clone eBioRDR5; eBioscience Inc., San Diego, CA), anti-PD-1–FITC (clone MIH4; eBioscience Inc., San Diego, CA), anti-CD3-V500 (clone SK7; Becton Dickinson Bioscience, San Jose, CA), anti-CD4-PerCP (clone SK3; Becton Dickinson Bioscience, San Jose, CA), anti-CD19-PerCP-cyanine 5.5 (Cy5.5) (clone SJ25C1; Becton Dickinson Bioscience, San Jose, CA), anti-CD45RA-APC (clone MEM-56; Exbio, Prague, Czech Republic), anti-C-C chemokine receptor type 7 (CCR7)-PE-Cy7 (clone G043H7; BioLegend, San Diego, CA), anti-CD28-Pacific blue (PB) (clone CD28.2; Exbio, Prague, Czech Republic), anti-gamma interferon (anti-IFN-γ)-FITC (clone 25723; R&D Systems, Minneapolis, MN), and anti-CD107a-Alexa Fluor 488 (AF488) (clone H4A3; BioLegend, San Diego, CA). The following unlabeled MAb were also used: TRAF1 rabbit anti-human immunoglobulin (clone 45D3; Cell Signaling, Boston, MA) and myeloid cell leukemia 1 protein (Mcl-1) rabbit anti-human immunoglobulin (clone Y37; Epitomics, Burlingame, CA). Goat anti-rabbit IgG-AF647 (Invitrogen, Carlsbad, CA) was used to develop primary unlabeled MAb. The following isotype controls were purchased: mouse IgG1-FITC (clone MOPC-21; BioLegend, San Diego, CA), mouse IgG1-Alexa Fluor 488 (AF488) (clone MOPC-21; BioLegend, San Diego, CA), and mouse IgG2b-FITC (clone 133303; R&D Systems, Minneapolis, MN).

Surface and intracellular phenotypic analysis. Peripheral HCV-specific CD8$^+$ cells were identified and quantified using pentamer staining as previously described (8). In patients with pentamer$^+$/CD8$^+$ cells detectable ex vivo, surface and intracellular staining for CD127, PD-1, Mcl-1, and TRAF1 was performed. Surface CD127 and PD-1 staining was carried out as previously reported (8). For Mcl-1 and TRAF1 studies, peripheral blood lymphocytes (PBL) were previously stimulated for 3 h with 2 μM specific peptide to induce antigen-specific protein expression. Harvested cells were first stained with pentamers, and then a combined staining for CD8 and intracellular molecules was performed using Cytofix/Cytoperm (Becton Dickinson Bioscience, San Jose, CA). Indirect labeling with rabbit anti-human MAb was used to detect Mcl-1 and TRAF1, followed by the further addition of AF647-conjugated goat anti-rabbit IgG. TRAF1 was also tested after 6 days of treatment with IL-7 (20 ng $\cdot$ ml^{-1}; eBioscience Inc., San Diego, CA) and after 48 h of treatment with TGF-β1 (5 ng $\cdot$ ml^{-1}; Invitrogen, Carlsbad, CA) in vitro, with β-galactosidase (2 μg $\cdot$ ml^{-1}; Santa Cruz Biotechnology, Santa Cruz, CA) being used as a negative control. TRAF1 was also longitudinally tested in two patients with PI subjected to anti-HCV treatment with DAA. For each sample, an aliquot stained with surface antigens and the intracellular secondary antibody was used as a negative control. In the rest of the stainings, appropriate isotype controls were used. For the degranulation assay and IFN-γ staining, PBL were challenged in vitro as previously described (9). Anti-CD107a-AF488 was added at the beginning of the stimulation. At the time of harvest, cells were stained with pentamer-PE and anti-CD8-PerCP, washed, and fixed and permeabilized using Cytofix/Cytoperm for subsequent intracellular staining with anti-IFN-γ–FITC. Stained cells were analyzed on a FACSCalibur flow cytometer using CellQuest software (Becton Dickinson Bioscience, San Jose, CA). In selected cases, an extended MAb panel (CD3-V500, CD28-PB, pentamer-PE, CD19-PerCP-Cy5 plus CD4-PerCP, CCR7-PE-Cy7, CD45RA-APC, CD8-APC-H7) was used to obtain a detailed description of the memory phenotype using a more sensitive detection method (43). These samples were acquired on a FACSCanto II flow cytometer (Becton Dickinson Bioscience, San Jose, CA) and analyzed using Infinicyt software (Cytognos, Spain). Phenotype comparisons were carried out using the mean fluorescence intensity (MFI) or the percentage of positive cells.

Specific T cell proliferation. For the *in vitro* stimulation experiments, 4-1BBL (Enzo Life Sciences, Farmingdale, NY), anti-programmed cell death protein ligand 1 (PD-L1) MAb (eBioscience Inc., San Diego, CA), IL-7 and IL-2 (R&D Systems, Minneapolis, MN), and β-galactosidase were purchased. PBL-specific *in vitro* challenge with the NS3$_{1406-1415}$, NS3$_{1073-1081}$, or CMV pp65$_{495-504}$ peptide was carried out as previously described (8). After specific *in vitro* expansion, TRAF1 expression by pentamer+/CD8+ cells from a number of patients was analyzed. PBL from selected patients with PI were also cultured with specific peptides in the presence of the following treatments: IL-7 (20 ng · ml^{-1}), 4-1BBL (1 μg · ml^{-1}), anti-PD-L1 blocking MAb (2 μg · ml^{-1}), β-galactosidase (2 μg · ml^{-1}), or the combinations IL-7 plus 4-1BBL and IL-7, 4-1BBL, and anti-PD-L1. Expansion was considered positive when the pentamer+/CD8+ cells were found in a cluster shape and the frequency of positive cells was at least 4 times higher than the *ex vivo* percentage with a minimum of 20 detectable dots.

TGF-β1 ELISA. The levels of active soluble TGF-β1 in serum from patients with RI and PI were measured using a commercial enzyme-linked immunosorbent assay (ELISA) kit (Quantikine ELISA human TGF-β1; R&D Systems, Minneapolis, MN), according to the manufacturer's instructions. The lower level of detection was 4.61 pg · ml^{-1}. In cases in which pentamer+/CD8+ cells were detectable *ex vivo*, the TGF-β1 level was correlated with TRAF1 expression. In patients with PI, the TGF-β1 level in the supernatant of PBL cultures was also tested at days 2 and 9 of the 10-day specific *in vitro* challenge to check TGF-β1 kinetics according to the expansion status.

Statistical analysis. Every epitope tested in each patient was considered an independent case. Quantitative and categorical variables are summarized as medians plus interquartile ranges (IQR) and as frequency distributions, respectively. Pearson's chi-square test, the Mann-Whitney U test, the Wilcoxon test, the Friedman test, the Spearman correlation test, and the linear trend test were employed where appropriate. All tests were two-tailed, and a P value of <0.05 was considered significant.

REFERENCES

1. Thimme R, Bukh J, Spangenberg HC, Wieland S, Pemberton J, Steiger C, Govindarajan S, Purcell RH, Chisari FV. 2002. Viral and immunological determinants of hepatitis C virus clearance, persistence, and disease. Proc Natl Acad Sci U S A 99:15661–15668. https://doi.org/10.1073/pnas.202608299.

2. Larrubia JR, Lokhande MU, Moreno-Cubero E, Garcia-Garzon S, Miquel J, Parra-Cid T, Gonzalez-Praetorious A, Perna C, Lazaro A, Sanz-de-Villalobos E. 2013. HCV-specific CD8+ cell detection at week 12 of chronic hepatitis C treatment with PEG-interferon-alpha2b/ribavirin correlates with infection resolution. Cell Immunol 286:31–38. https://doi.org/10.1016/j.cellimm.2013.11.001.

3. Martin B, Hennecke N, Lohmann V, Kayser A, Neumann-Haefelin C, Kukolj G, Bocher WO, Thimme R. 2014. Restoration of HCV-specific CD8+ T cell function by interferon-free therapy. J Hepatol 61:538–543. https://doi.org/10.1016/j.jhep.2014.05.043.

4. Veerapu NS, Raghuraman S, Liang TJ, Heller T, Rehermann B. 2011. Sporadic reappearance of minute amounts of hepatitis C virus RNA after successful therapy stimulates cellular immune responses. Gastroenterology 140:676–685.e1. https://doi.org/10.1053/j.gastro.2010.10.048.

5. Gambato M, Perez-Del-Pulgar S, Hedskog C, Svarovskia ES, Brainard D, Denning J, Curry MP, Charlton M, Caro-Perez N, Londono MC, Koutsoudakis G, Forns X. 2016. Hepatitis C virus RNA persists in liver explants of most patients awaiting liver transplantation treated with an interferon-free regimen. Gastroenterology 151:633–636.e3. https://doi.org/10.1053/j.gastro.2016.06.025.

6. Klepper A, Eng FJ, Doyle EH, El-Shamy A, Rahman AH, Fiel MI, Avino GC, Lee M, Ye F, Roayaie S, Bansal MB, MacDonald MR, Schiano TD, Branch AD. 2017. Hepatitis C virus double-stranded RNA is the predominant form in human liver and in interferon-treated cells. Hepatology 66:357–370. https://doi.org/10.1002/hep.28846.

7. Veerapu NS, Park SH, Tully DC, Allen TM, Rehermann B. 2014. Trace amounts of sporadically reappearing HCV RNA can cause infection. J Clin Invest 124:3469–3478. https://doi.org/10.1172/JCI73104.

8. Larrubia JR, Benito-Martinez S, Miquel J, Calvino M, Sanz-de-Villalobos E,

Gonzalez-Praetorius A, Albertos S, Garcia-Garzon S, Lokhande M, Parra-Cid T. 2011. Bim-mediated apoptosis and PD-1/PD-L1 pathway impair reactivity of PD1(+)/CD127(−) HCV-specific CD8(+) cells targeting the virus in chronic hepatitis C virus infection. Cell Immunol 269:104–114. https://doi.org/10.1016/j.cellimm.2011.03.011.

9. Larrubia JR, Lokhande MU, Garcia-Garzon S, Miquel J, Gonzalez-Praetorius A, Parra-Cid T, Sanz-de-Villalobos E. 2013. Persistent hepatitis C virus (HCV) infection impairs HCV-specific cytotoxic T cell reactivity through Mcl-1/Bim imbalance due to CD127 down-regulation. J Viral Hepat 20:85–94. https://doi.org/10.1111/j.1365-2893.2012.01618.x.

10. Radziewicz H, Ibegbu CC, Hon H, Osborn MK, Obideen K, Wehbi M, Freeman GJ, Lennox JL, Workowski KA, Hanson HL, Grakoui A. 2008. Impaired hepatitis C virus (HCV)-specific effector CD8⁺ T cells undergo massive apoptosis in the peripheral blood during acute HCV infection and in the liver during the chronic phase of infection. J Virol 82:9808–9822. https://doi.org/10.1128/JVI.01075-08.

11. Bengsch B, Seigel B, Ruhl M, Timm J, Kuntz M, Blum HE, Pircher H, Thimme R. 2010. Coexpression of PD-1, 2B4, CD160 and KLRG1 on exhausted HCV-specific CD8⁺ T cells is linked to antigen recognition and T cell differentiation. PLoS Pathog 6:e1000947. https://doi.org/10.1371/journal.ppat.1000947.

12. McMahan RH, Golden-Mason L, Nishimura MI, McMahon BJ, Kemper M, Allen TM, Gretch DR, Rosen HR. 2010. Tim-3 expression on PD-1⁺ HCV-specific human CTLs is associated with viral persistence, and its blockade restores hepatocyte-directed in vitro cytotoxicity. J Clin Invest 120:4546–4557. https://doi.org/10.1172/JCI43127.

13. Fisicaro P, Valdatta C, Massari M, Loggi E, Ravanetti L, Urbani S, Giuberti T, Cavalli A, Vandelli C, Andreone P, Missale G, Ferrari C. 2012. Combined blockade of programmed death-1 and activation of CD137 increase responses of human liver T cells against HBV, but not HCV. Gastroenterology 143:1576–1585.e4. https://doi.org/10.1053/j.gastro.2012.08.041.

14. Utzschneider DT, Charmoy M, Chennupati V, Pousse L, Ferreira DP, Calderon-Copete S, Danilo M, Alfei F, Hofmann M, Wieland D, Prader-vand S, Thimme R, Zehn D, Held W. 2016. T cell factor 1-expressing memory-like CD8(+) T cells sustain the immune response to chronic viral infections. Immunity 45:415–427. https://doi.org/10.1016/j.immuni.2016.07.021.

15. Im SJ, Hashimoto M, Gerner MY, Lee J, Kissick HT, Burger MC, Shan Q, Hale JS, Lee J, Nasti TH, Sharpe AH, Freeman GJ, Germain RN, Nakaya HI, Xue HH, Ahmed R. 2016. Defining CD8⁺ T cells that provide the proliferative burst after PD-1 therapy. Nature 537:417–421. https://doi.org/10.1038/nature19330.

16. Paley MA, Kroy DC, Odorizzi PM, Johnnidis JB, Dolfi DV, Barnett BE, Bikoff EK, Robertson EJ, Lauer GM, Reiner SL, Wherry EJ. 2012. Progenitor and terminal subsets of CD8⁺ T cells cooperate to contain chronic viral infection. Science 338:1220–1225. https://doi.org/10.1126/science.1229620.

17. Wieland D, Kemming J, Schuch A, Emmerich F, Knolle P, Neumann-Haefelin C, Held W, Zehn D, Hofmann M, Thimme R. 2017. TCF1⁺ hepatitis C virus-specific CD8⁺ T cells are maintained after cessation of chronic antigen stimulation. Nat Commun 8:15050. https://doi.org/10.1038/ncomms15050.

18. He XS, Rehermann B, Lopez-Labrador FX, Boisvert J, Cheung R, Mumm J, Wedemeyer H, Berenguer M, Wright TL, Davis MM, Greenberg HB. 1999. Quantitative analysis of hepatitis C virus-specific CD8(+) T cells in peripheral blood and liver using peptide-MHC tetramers. Proc Natl Acad Sci U S A 96:5692–5697. https://doi.org/10.1073/pnas.96.10.5692.

19. Kober J, Leitner J, Klauser C, Woitek R, Majdic O, Stockl J, Herndler-Brandstetter D, Grubeck-Loebenstein B, Reipert BM, Pickl WF, Pfistershammer K, Steinberger P. 2008. The capacity of the TNF family members 4-1BBL, OX40L, CD70, GITRL, CD30L and LIGHT to costimulate human T cells. Eur J Immunol 38:2678–2688. https://doi.org/10.1002/eji.200838250.

20. McPherson AJ, Snell LM, Mak TW, Watts TH. 2012. Opposing roles for TRAF1 in the alternative versus classical NF-kappaB pathway in T cells. J Biol Chem 287:23010–23019. https://doi.org/10.1074/jbc.M112.350538.

21. Schwenzer R, Siemienski K, Liptay S, Schubert G, Peters N, Scheurich P, Schmid RM, Wajant H. 1999. The human tumor necrosis factor (TNF) receptor-associated factor 1 gene (TRAF1) is up-regulated by cytokines of the TNF ligand family and modulates TNF-induced activation of NF-kappaB and c-Jun N-terminal kinase. J Biol Chem 274:19368–19374. https://doi.org/10.1074/jbc.274.27.19368.

22. Lee SY, Choi Y. 2007. TRAF1 and its biological functions. Adv Exp Med Biol 597:25–31. https://doi.org/10.1007/978-0-387-70630-6_2.

23. Wang C, McPherson AJ, Jones RB, Kawamura KS, Lin GH, Lang PA, Ambagala T, Pellegrini M, Calzascia T, Aidarus N, Elford AR, Yue FY,

Kremmer E, Kovacs CM, Benko E, Tremblay C, Routy JP, Bernard NF, Ostrowski MA, Ohashi PS, Watts TH. 2012. Loss of the signaling adaptor TRAF1 causes CD8⁺ T cell dysregulation during human and murine chronic infection. J Exp Med 209:77–91. https://doi.org/10.1084/jem.20110675.

24. Alatrakchi N, Graham CS, van der Vliet HJ, Sherman KE, Exley MA, Koziel MJ. 2007. Hepatitis C virus (HCV)-specific CD8⁺ cells produce transforming growth factor beta that can suppress HCV-specific T-cell responses. J Virol 81:5882–5892. https://doi.org/10.1128/JVI.02202-06.

25. Kim JH, Lee CH, Lee SW. 2016. Hepatitis C virus infection stimulates transforming growth factor-beta1 expression through up-regulating miR-192. J Microbiol 54:520–526. https://doi.org/10.1007/s12275-016-6240-3.

26. Hall CH, Kassel R, Tacke RS, Hahn YS. 2010. HCV⁺ hepatocytes induce human regulatory CD4⁺ T cells through the production of TGF-beta. PLoS One 5:e12154. https://doi.org/10.1371/journal.pone.0012154.

27. Pellegrini M, Calzascia T, Toe JG, Preston SP, Lin AE, Elford AR, Shahinian A, Lang PA, Lang KS, Morre M, Assouline B, Lahl K, Sparwasser T, Tedder TF, Paik JH, DePinho RA, Basta S, Ohashi PS, Mak TW. 2011. IL-7 engages multiple mechanisms to overcome chronic viral infection and limit organ pathology. Cell 144:601–613. https://doi.org/10.1016/j.cell.2011.01.011.

28. Terrault NA, Zeuzem S, Di Bisceglie AM, Lim JK, Pockros PJ, Frazier LM, Kuo A, Lok AS, Shiffman ML, Ben Ari Z, Akushevich L, Vainorius M, Sulkowski MS, Fried MW, Nelson DR, HCV-TARGET Study Group. 2016. Effectiveness of ledipasvir-sofosbuvir combination in patients with hepatitis C virus infection and factors associated with sustained virologic response. Gastroenterology 151:1131–1140.e5. https://doi.org/10.1053/j.gastro.2016.08.004.

29. Kamphorst AO, Wieland A, Nasti T, Yang S, Zhang R, Barber DL, Konieczny BT, Daugherty CZ, Koenig L, Yu K, Sica GL, Sharpe AH, Freeman GJ, Blazar BR, Turka LA, Owonikoko TK, Pillai RN, Ramalingam SS, Araki K, Ahmed R. 2017. Rescue of exhausted CD8 T cells by PD-1-targeted therapies is CD28-dependent. Science 355:1423–1427. https://doi.org/10.1126/science.aaf0683.

30. Freeman BE, Hammarlund E, Raue HP, Slifka MK. 2012. Regulation of innate CD8⁺ T-cell activation mediated by cytokines. Proc Natl Acad Sci U S A 109:9971–9976. https://doi.org/10.1073/pnas.1203543109.

31. Grayson JM, Weant AE, Holbrook BC, Hildeman D. 2006. Role of Bim in regulating CD8⁺ T-cell responses during chronic viral infection. J Virol 80:8627–8638. https://doi.org/10.1128/JVI.00855-06.

32. Cox AL, Mosbruger T, Mao Q, Liu Z, Wang XH, Yang HC, Sidney J, Sette A, Pardoll D, Thomas DL, Ray SC. 2005. Cellular immune selection with hepatitis C virus persistence in humans. J Exp Med 201:1741–1752. https://doi.org/10.1084/jem.20050121.

33. Tinoco R, Alcalde V, Yang Y, Sauer K, Zuniga EI. 2009. Cell-intrinsic transforming growth factor-beta signaling mediates virus-specific CD8⁺ T cell deletion and viral persistence in vivo. Immunity 31:145–157. https://doi.org/10.1016/j.immuni.2009.06.015.

34. Wang C, Wen T, Routy JP, Bernard NF, Sekaly RP, Watts TH. 2007. 4-1BBL induces TNF receptor-associated factor 1-dependent Bim modulation in human T cells and is a critical component in the costimulation-dependent rescue of functionally impaired HIV-specific CD8 T cells. J Immunol 179:8252–8263. https://doi.org/10.4049/jimmunol.179.12.8252.

35. Sabbagh L, Srokowski CC, Pulle G, Snell LM, Sedgmen BJ, Liu Y, Tsitsikov EN, Watts TH. 2006. A critical role for TNF receptor-associated factor 1 and Bim down-regulation in CD8 memory T cell survival. Proc Natl Acad Sci U S A 103:18703–18708. https://doi.org/10.1073/pnas.0602919103.

36. Larrubia JR, Moreno-Cubero E, Lokhande MU, Garcia-Garzon S, Lazaro A, Miquel J, Perna C, Sanz-de-Villalobos E. 2014. Adaptive immune response during hepatitis C virus infection. World J Gastroenterol 20:3418–3430. https://doi.org/10.3748/wjg.v20.i13.3418.

37. Owusu Sekyere S, Suneetha PV, Kraft AR, Zhang S, Dietz J, Sarrazin C, Manns MP, Schlaphoff V, Cornberg M, Wedemeyer H. 2015. A heterogeneous hierarchy of co-regulatory receptors regulates exhaustion of HCV-specific CD8 T cells in patients with chronic hepatitis C. J Hepatol 62:31–40. https://doi.org/10.1016/j.jhep.2014.08.008.

38. Soderholm J, Ahlen G, Kaul A, Frelin L, Alheim M, Barnfield C, Liljestrom P, Weiland O, Milich DR, Bartenschlager R, Sallberg M. 2006. Relation between viral fitness and immune escape within the hepatitis C virus protease. Gut 55:266–274. https://doi.org/10.1136/gut.2005.072231.

39. Gaudieri S, Rauch A, Park LP, Freitas E, Herrmann S, Jeffrey G, Cheng W, Pfafferott K, Naidoo K, Chapman R, Battegay M, Weber R, Telenti A, Furrer H, James I, Lucas M, Mallal SA. 2006. Evidence of viral adaptation

to HLA class I-restricted immune pressure in chronic hepatitis C virus infection. J Virol 80:11094–11104. https://doi.org/10.1128/JVI.00912-06.

40. Kelly C, Swadling L, Brown A, Capone S, Folgori A, Salio M, Klenerman P, Barnes E. 2015. Cross-reactivity of hepatitis C virus specific vaccine-induced T cells at immunodominant epitopes. Eur J Immunol 45: 309–316. https://doi.org/10.1002/eji.201444686.

41. Nowak MA, Bangham CR. 1996. Population dynamics of immune responses to persistent viruses. Science 272:74–79. https://doi.org/10.1126/science.272.5258.74.

42. Poynard T, Bedossa P, Opolon P. 1997. Natural history of liver fibrosis progression in patients with chronic hepatitis C. The OBSVIRC, METAVIR, CLINIVIR, and DOSVIRC groups. Lancet 349:825–832.

43. Paiva B, van Dongen JJ, Orfao A. 2015. New criteria for response assessment: role of minimal residual disease in multiple myeloma. Blood 125: 3059–3068. https://doi.org/10.1182/blood-2014-11-568907.

44. Mahnke YD, Brodie TM, Sallusto F, Roederer M, Lugli E. 2013. The who's who of T-cell differentiation: human memory T-cell subsets. Eur J Immunol 43:2797–2809. https://doi.org/10.1002/eji.201343751.

45. Hui E, Cheung J, Zhu J, Su X, Taylor MJ, Wallweber HA, Sasmal DK, Huang J, Kim JM, Mellman I, Vale RD. 2017. T cell costimulatory receptor CD28 is a primary target for PD-1-mediated inhibition. Science 355:1428–1433. https://doi.org/10.1126/science.aaf1292.

46. Chang JH, Kim YJ, Han SH, Kang CY. 2009. IFN-gamma-STAT1 signal regulates the differentiation of inducible Treg: potential role for ROS-mediated apoptosis. Eur J Immunol 39:1241–1251. https://doi.org/10.1002/eji.200838913.

47. Bolacchi F, Sinistro A, Ciaprini C, Demin F, Capozzi M, Carducci FC, Drapeau CM, Rocchi G, Bergamini A. 2006. Increased hepatitis C virus (HCV)-specific CD4+CD25+ regulatory T lymphocytes and reduced HCV-specific CD4+ T cell response in HCV-infected patients with normal versus abnormal alanine aminotransferase levels. Clin Exp Immunol 144: 188–196. https://doi.org/10.1111/j.1365-2249.2006.03048.x.

48. Shin H, Blackburn SD, Blattman JN, Wherry EJ. 2007. Viral antigen and extensive division maintain virus-specific CD8 T cells during chronic infection. J Exp Med 204:941–949. https://doi.org/10.1084/jem.20061937.

49. Pauken KE, Sammons MA, Odorizzi PM, Manne S, Godec J, Khan O, Drake AM, Chen Z, Sen DR, Kurachi M, Barnitz RA, Bartman C, Bengsch B, Huang AC, Schenkel JM, Vahedi G, Haining WN, Berger SL, Wherry EJ. 2016. Epigenetic stability of exhausted T cells limits durability of reinvigoration by PD-1 blockade. Science 354:1160–1165. https://doi.org/10.1126/science.aaf2807.

50. Li S, Vriend LE, Nasser IA, Popov Y, Afdhal NH, Koziel MJ, Schuppan D, Exley MA, Alatrakchi N. 2012. Hepatitis C virus-specific T-cell-derived transforming growth factor beta is associated with slow hepatic fibrogenesis. Hepatology 56:2094–2105. https://doi.org/10.1002/hep.25951.

51. Chen ZW, Li H, Ren H, Hu P. 2016. Global prevalence of pre-existing HCV variants resistant to direct-acting antiviral agents (DAAs): mining the GenBank HCV genome data. Sci Rep 6:20310. https://doi.org/10.1038/srep20310.

52. Manns MP, Buti M, Gane E, Pawlotsky JM, Razavi H, Terrault N, Younossi Z. 2017. Hepatitis C virus infection. Nat Rev Dis Primers 3:17006. https://doi.org/10.1038/nrdp.2017.6.

53. Bedossa P, Poynard T. 1996. An algorithm for the grading of activity in chronic hepatitis C. The METAVIR Cooperative Study Group. Hepatology 24:289–293.